Available online at www.sciencedirect.com
ScienceDirect
Organic Geochemistry 37 (2006) 1052–1073
Organic Geochemistry
www.elsevier.com/locate/orggeochem

Preservation of carbohydrates through sulfurization in a Jurassic euxinic shelf sea: Examination of the Blackstone Band TOC cycle in the Kimmeridge Clay Formation, UK

Bart E. van Dongen [1], Stefan Schouten, Jaap S. Sinninghe Damsté *

Department of Marine Biogeochemistry and Toxicology, Royal Netherlands Institute for Sea Research (NIOZ), P.O. Box 59, 1790 AB Den Burg, Texel, The Netherlands

Received 9 May 2006; accepted 17 May 2006
Available online 7 July 2006

Abstract

A complete total organic carbon (TOC) cycle in the Upper Jurassic Kimmeridge Clay Formation (KCF) comprising the extremely TOC-rich (34%) Blackstone Band was studied to investigate the controlling factors on TOC accumulation. Compared with the under- and overlying strata, TOC in the Blackstone Band was enriched by a factor of six and, concomitantly, the $\delta^{13}C_{TOC}$ shows a $\sim$4‰ enrichment. Al-normalized TOC values indicated that the enhanced TOC values were probably caused by increased TOC accumulation and not by a decreased dilution with inorganic matter. The amounts of short chain alkylated thiophenes and the sulfur-rich unresolved complex mixture (UCM) in the kerogen pyrolysates, as well as the TOC/Al ratios, correlated linearly with $\delta^{13}C_{TOC}$ for sediments with TOC/Al ratios >1.7. The alkylated thiophenes and sulfur-rich UCM both originate from sulfurized carbohydrate carbon (C_{carb}), suggesting that the primary cause of the TOC maximum is the enhanced contribution of C_{carb} to TOC. Since carbohydrates can be substantially ^{13}C-enriched over lipids in biomass, the enhanced contribution of C_{carb} explains the enriched $\delta^{13}C_{TOC}$ values. Compound specific isotope data showed that primary productivity during deposition of the KCF TOC cycle varied little, while a two member isotopic mixing model showed that the preservation of C_{carb} relative to that of the lipid carbon may have increased by a factor of >10 in the Blackstone Band. The enhanced preservation of C_{carb} was most likely caused by more frequent or longer lasting events of photic zone euxinia, as revealed by the concentration of isorenieratene derivatives. Enhanced contributions of C_{carb} have also been observed in other KCF cycles, suggesting that enhanced preservation of C_{carb}, rather than an increase in primary production, exerted direct control on the TOC cycles of the KCF.

1. Introduction

Many studies have been devoted to the nature of the organic matter (OM) distribution in the geological record and a key question remains as to which factors, such as primary OM productivity and preservation/degradation, are crucial in determining OM accumulation. Specifically, the controls on OM

* Corresponding author.
E-mail address: damste@nioz.nl (J.S. Sinninghe Damsté).
[1] Present address: Institute for Applied Environmental Research, Stockholm University, 10691 Stockholm, Sweden.

0146-6380/$ - see front matter © 2006 Elsevier Ltd. All rights reserved.
doi:10.1016/j.orggeochem.2006.05.007

accumulation in OM-rich marine sediments have been a topic of interest to biogeochemists and petroleum geologists, as these sediments are often potential oil source rocks. Prime examples of such sulfur (S)- and OM-rich sediments can be found in the Kimmeridge Clay Formation (KCF), the presumed source rock of most North Sea oils (Cooper et al., 1995; Miller, 1989; Tyson, 1996; Wignall, 1994a).

The KCF was deposited in a series of basins that extended from eastern Greenland and Canada to offshore Norway and south to the English Channel (Doré et al., 1985). It was shown that, onshore, the sediments display a cyclic alternation of mudstones, bituminous shales, oil shales and carbonates, with TOC contents up to values as high as 60% (i.e. substantially consisting of OM; van Kaam-Peters et al., 1998), but individual cycles vary in thickness and are not always complete (Tyson, 1989). The mean TOC content of the >500 m thick KCF in southern Dorset (UK) is 4.2% (Tyson, 2004). An intriguing positive correlation has been observed between TOC and $\delta^{13}C_{TOC}$ (Huc et al., 1992; van Kaam-Peters et al., 1998; Sinninghe Damsté et al., 1998; Sælen et al., 2000). Numerous studies have reconstructed the palaeoceanographic conditions responsible for deposition of the sediments and postulated models to explain their enhanced TOC content as well as the correlation between TOC content and $\delta^{13}C_{TOC}$ (e.g., Tyson et al., 1979; Cox and Gallois, 1981; Oschmann, 1988, 1991; Miller, 1989; Huc et al., 1992; Hollander et al., 1993; Wignall, 1994a,b; Tyson, 1996; van Kaam-Peters et al., 1998; Sælen et al., 2000). Some of the models assume that these enhanced TOC values result from increased primary production (e.g., Oschmann, 1988; Huc et al., 1992; Bertrand and Lallier-Vergès, 1993; Herbin et al., 1993; Ramanampisoa and Disnar, 1994; Boussafir et al., 1995; Lallier-Vergès et al., 1997; Sælen et al., 2000); other models suggest enhanced preservation as the primary cause (Tyson et al., 1979; van Kaam-Peters et al., 1997, 1998; Sinninghe Damsté et al., 1998), whilst in various models both factors play a role (Tyson, 1996; Tribovillard et al., 2001).

The "productivity" end member model explains the deposition of TOC-rich sediments by the relatively high position of the chemocline and the resulting turbulent entrainment of nutrients, which would lead to high primary production. Increased primary productivity may result in decreased isotopic fractionation during photosynthesis, so a shift similar to that observed for the $\delta^{13}C_{TOC}$ would be expected for the $\delta^{13}C$ values of biomarkers derived from primary producers. However, no shift in the $\delta^{13}C$ values of any of the algal and bacterial biomarkers was observed (van Kaam-Peters et al., 1998; Sinninghe Damsté et al., 1998), suggesting that substantially increased primary production cannot be the major cause of the increase in TOC content.

The "preservation" end member model explains the deposition of TOC-rich sediments primarily by a decreased remineralization of the downward flux of OM-rich particles. Boussafir et al. (1995) found, using transmission electron microscopy, that sulfurization of OM by inorganic sulfur could play an important role in the preservation of OM. These authors suggested that primary production, sulfate reduction intensity and lipid sulfurization likely all played a major role in the variation in TOC. The organic S concentrations vary throughout the KCF and, based on the increasing abundance of organic S with increasing TOC (and $\delta^{13}C_{TOC}$), van Kaam-Peters et al. (1998) suggested that TOC was controlled by the degree of sulfurization of OM and van Kaam-Peters et al. (1997, 1998) reported that, with increasing TOC, ^{13}C-enriched short chain alkylated thiophenes became increasingly abundant in the pyrolysate of KCF rock samples. In addition, the material formed upon sulfurization of carbohydrates yields high amounts of organic sulfur compounds (OSCs) upon pyrolysis (Sinninghe Damsté et al., 1998; Kok et al., 2000b; van Dongen et al., 2003a). These products were mainly short chain alkyl thiophenes, compounds similar to the OSCs found in the KCF pyrolysates, suggesting that the isotopically enriched short chain thiophenes in the latter are probably derived from S-bound carbohydrates in the kerogen (van Kaam-Peters et al., 1998); van Dongen et al. (2003b) showed that the unresolved complex mixture (UCM), present in large amounts in pyrolysates of KCF sediments, also had its primary origin in the preservation of carbohydrates through natural sulfurization, providing further evidence for the enhanced preservation model as a major mechanism for OM accumulation. Carbohydrates can be enriched in ^{13}C (up to 16‰) relative to the lipids in biomass (Deines, 1980; Sinninghe Damsté et al., 2001b; van Dongen et al., 2002). This indicates that the differences in the degree of preservation of labile carbohydrate carbon through sulfurization may explain the high ^{13}C contents of short chain alkylated thiophenes in KCF kerogen pyrolysates and the large range in $\delta^{13}C_{TOC}$ encountered in the KCF.

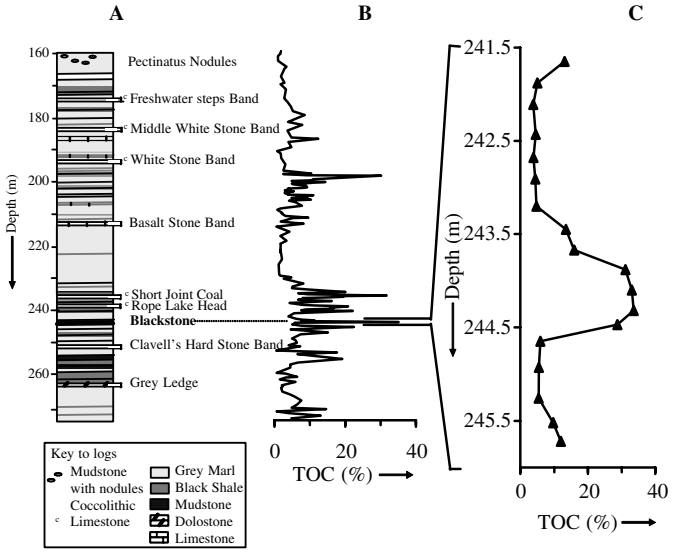

Fig. 1. (A) General vertical section of Upper Kimmeridge Clay in Dorset, (B) TOC values and (C) enlargement of TOC profile around Blackstone Band (lithology according to Morgans-Bell et al., 2001).

Our initial detailed organic geochemical work (van Kaam-Peters et al., 1998) was performed on a suite of outcrop samples covering a long period in time (approximately 1.5 Ma) and so did not focus on the mechanism for the observed TOC cyclicity in the KCF in relation to the $\delta^{13}C_{TOC}$ enrichment. The KCF covers a large number of TOC cycles (Morgans-Bell et al., 2001). We have therefore now examined a selected set of sediments taken from a core section covering a single TOC cycle, around the Blackstone Band, the richest oil shale bed of the KCF, with extremely high TOC content (Morgans-Bell et al., 2001; Fig. 1). The results suggest that enhanced preservation of carbohydrates through sulfurization, rather than primary productivity, exerts a primary control on TOC accumulation and the $\delta^{13}C_{TOC}$ values in this and, possibly other, TOC cycles in the KCF.

2. Experimental

2.1. Sample description

Samples were obtained from a core from the Swanworth Quarry 1 borehole [SY 9675 7823], South Dorset, UK. This core was drilled as part of the UK Natural Environment Research Council's Rapid Global Geological Events special topic 'Anatomy of a Source Rock'. A complete description of the core is given by Morgans-Bell et al. (2001). Eighteen samples were taken, at approximately 20 cm intervals, from 241.7 m to 245.7 m depth (Table 1) including the Blackstone Band interval (Fig. 1). In a package of OM-rich shales that straddle Bed group 42 (the *Pectinatites wheatleyenesis–Pectinatites hudlestoni* zonal boundary; Morgans-Bell et al., 2001) the Blackstone forms the most prominent bed. It is a dark brown, laminated, highly OM-rich, weakly fissile mudstone containing pyritic nodules and shelly material (Fig. 1). In contrast, directly above it rests a series of olive-grey organic rich, coccolithic mudstones (weakly laminated in part) and below lies a bed rich in pyritized specimens of the planktonic cinoid *Saccocoma*. The sediments were freeze dried and stored frozen (−20 °C) prior to use.

2.2. Extraction and fractionation

The Soxhlet extractions, asphaltenes removal and separation of the maltene fractions into saturated hydrocarbon, aromatic hydrocarbon and polar fractions were performed as described previously (van Kaam-Peters et al., 1998), and a mixture of four standards (3-methyl-5,5-d_2-heneicosane, 2,3-dimethyl5-(1′,1′-d_2-hexadecyl)thiophene, 2-methyl-2-(4,8,12-trimethyltridecyl)chroman, 2,3-dimethyl-5-(1′,1′-d_2-hexadecyl)thiolane) was added to the total extract for quantitative analysis (Kohnen et al., 1990). Further cleaning of the saturated hydrocarbon fractions was performed with column chromatography using a column (5 cm × 1 cm) packed with

Table 1
Depth, TOC, $\delta^{13}C_{TOC}$, carbonate concentration and XRF data for samples

Sample	Depth (m)	TOC (%)	$\delta^{13}C_{TOC}$ (‰)	Carbonate (%)	Al_2O_3 (%)	SiO_2 (%)	TiO_2 (%)	Ni (ppm)
KCF1	241.7	13.1	−23.1	24.7	13.5	34.1	0.59	82
KCF2	241.9	5.0	−25.0	21.3	16.0	43.7	0.73	55
KCF3	242.1	3.8	−25.6	19.0	16.8	45.5	0.78	56
KCF4	242.4	4.5	−24.5	13.1	15.8	52.1	0.84	48
KCF5	242.7	4.4	−24.4	14.7	15.6	52.5	0.86	48
KCF6	242.9	3.9	−24.5	13.3	15.3	51.8	0.84	46
KCF7	243.2	4.7	−25.1	15.8	16.2	49.3	0.83	50
KCF8	243.5	13.5	−23.9	18.1	15.0	38.9	0.71	72
KCF9	243.7	15.9	−23.5	17.4	13.5	34.9	0.60	94
KCF10	243.9	31.1	−22.9	15.3	9.0	23.5	0.43	66
KCF11	244.1	33.1	−21.3	24.8	5.9	15.5	0.31	64
KCF12	244.3	33.6	−21.1	32.6	4.0	10.0	0.20	68
KCF13	244.5	28.7	−21.9	27.8	7.3	19.6	0.37	66
KCF14	244.7	5.9	−25.0	40.5	10.1	30.9	0.51	57
KCF15	244.9	5.5	−25.7	22.4	13.9	45.7	0.75	50
KCF16	245.3	5.4	−26.0	19.3	13.9	48.8	0.78	53
KCF17	245.5	9.7	−26.2	20.1	14.4	42.6	0.74	80
KCF18	245.7	12.0	−26.8	16.3	16.2	39.2	0.69	124

Ag^+-impregnated silica by elution with hexane (20 ml). The fractions obtained were analyzed using gas chromatography (GC), gas chromatography–mass spectrometry (GC/MS), and, in selected cases, isotope-ratio-monitoring GC/MS (irm-GC/MS) as described below. The residues after extraction were dried and used for Curie-point pyrolysis-gas chromatography/flame ionization detection (Py-GC/FID) and Curie-point pyrolysis-gas chromatography/mass spectrometry (Py-GC/MS).

2.3. Instrumental analysis

Carbonate contents were determined by weighing the dry sediments before and after decalcification (1 M HCl at room temperature). TOC contents were determined with a Fisons Instruments NCS-1500 Elemental Analyzer using flash combustion at 1030 °C. The $\delta^{13}C$ values (vs. VPDB standard) were measured on bulk sediments, after removal of the inorganic carbonate with diluted 1 M HCl at room temperature for 16 h on the same machine connected to a Thermofinnigan Delta^{Plus} mass spectrometer via a ConFlo Interface. CO_2 was used as the reference gas. The standard deviation of replicate measurements was always better than 0.2‰ vs. VPDB.

GC, GC/MS and irm-GC/MS were carried out as described previously (van Kaam-Peters et al., 1997). Py-GC/FID and Py-GC/MS were conducted with a Hewlett-Packard 5890 gas chromatograph using a FOM-5LX or FOM-4LX unit, respectively, for pyrolysis. The powdered samples were pressed on a flattened ferromagnetic wire with a Curie-point temperature of 610 °C. The same conditions were used as described previously (van Kaam-Peters et al., 1997). In the case of the measurement of the UCM of the flash pyrolysate the gas chromatograph was programmed from 0 °C (5 min) to 300 °C (20 min) at a rate of 6 °C/min.

The samples were ground and homogenized in an agate ball mill prior to analysis by X-ray fluorescence (XRF) at the University of Oldenburg. Ca. 600 mg of the powder was mixed with 3.6 g of $Li_2B_4O_7$ and pre-oxidized at 500 °C for 5 h followed by the addition of 1 g of NH_4NO_4 and heating at 500 °C for 4 h. The samples were melted at 1200 °C in platinum crucibles and cooled in platinum disc moulds. The disks were analyzed with a Philips PW 2400 X-ray spectrometer and analytical precision was verified by preparation and analysis of several in-house and international standards. Precision and accuracy were better than 2%.

2.4. Quantification

The most abundant *n*-alkanes, pristane and phytane were quantified by comparing the peak areas in the FID trace with that of the internal *n*-alkane standard. The remaining *n*-alkanes and 3-isopropyltetracosane (**I**; see Appendix for structures) were quantified by integrating their peak areas in the *m/z* 57 mass chromatogram and comparison with

the peak area of the C_{23} *n*-alkane with known concentration. The concentrations of the most abundant derivatives of isorenieratene (**II**–**XVI**), 5α-cholestane (**XVII**), 4-methyl-5α-steranes (**XVII**) and the C_{30}–C_{31} hopanes (**XIX**–**XX**) were determined as described previously (van Kaam-Peters et al., 1998; Sinninghe Damsté et al., 2001a). The C_{29}–C_{30} neohop-13(18)-enes (**XXI**–**XXII**) and C_{25}–C_{26} aromatic hopanoids (**XXIII**–**XXIV**) were quantified by integrating the peak areas in the *m*/*z* 191 (neohopenes), 328 (hopanoid **XXIV**) or 346 (hopanoid **XXIII**) chromatograms and comparison with the C_{23} *n*-alkane in the *m*/*z* 57 mass chromatogram. The concentrations were corrected for the different relative intensities of the fragment ions, using correction factors determined from mass spectra of pure compounds.

The 2,3-dimethylthiophene to (1,2-dimethylbenzene + *n*-non-1-ene) ratio (Eglinton et al., 1990), the 2-methylthiophene to toluene ratio, the 2-ethylthiophene + 2,5-dimethylthiophene to (2-ethylthiophene + 2,5-dimethylthiophene + 2,4-dimethylthiophene + 2,3-dimethylthiopene) and the ratio of benzothiophenes to toluene in kerogen pyrolysates were calculated as described by van Kaam-Peters et al. (1998). The ratio of UCM over C_{18} to C_{27} *n*-alkanes and *n*-alkenes was calculated from the area of the UCM corrected for bleeding of the stationary phase from the capillary column and the peak areas of the C_{18} to C_{27} *n*-alkanes and *n*-alkenes in the FID trace.

3. Results

3.1. Bulk analysis

The TOC and carbonate content of the sediments ranged from 4% to 34% (Fig. 2) and 15% to 41%, respectively (Table 1). The TOC contents showed a systematic variation with depth, peaking at 244.3 m in the Blackstone Band (Fig. 2). The $\delta^{13}C_{TOC}$ values ranged from −21‰ to −27‰ with the most ^{13}C enriched values corresponding to peak TOC values (Fig. 2). The Al_2O_3, SiO_2, TiO_2 and Ni contents are listed in Table 1 and all, except Ni, showed minimum values at peak TOC content (Table 1).

3.2. Extractable organic matter

3.2.1. Free acyclic hydrocarbons

The saturated hydrocarbon fractions were all dominated by *n*-alkanes, pristane and phytane. The concentration (normalized to TOC) of pristane, phytane, 3-isopropyltetracosane (**I**), C_{21} and C_{23} *n*-alkanes, as well as the summed concentration of the C_{16}–C_{35} (except C_{21} and C_{23}) *n*-alkanes, showed a minimum in the 243.5–244.5 m interval (Fig. 2),

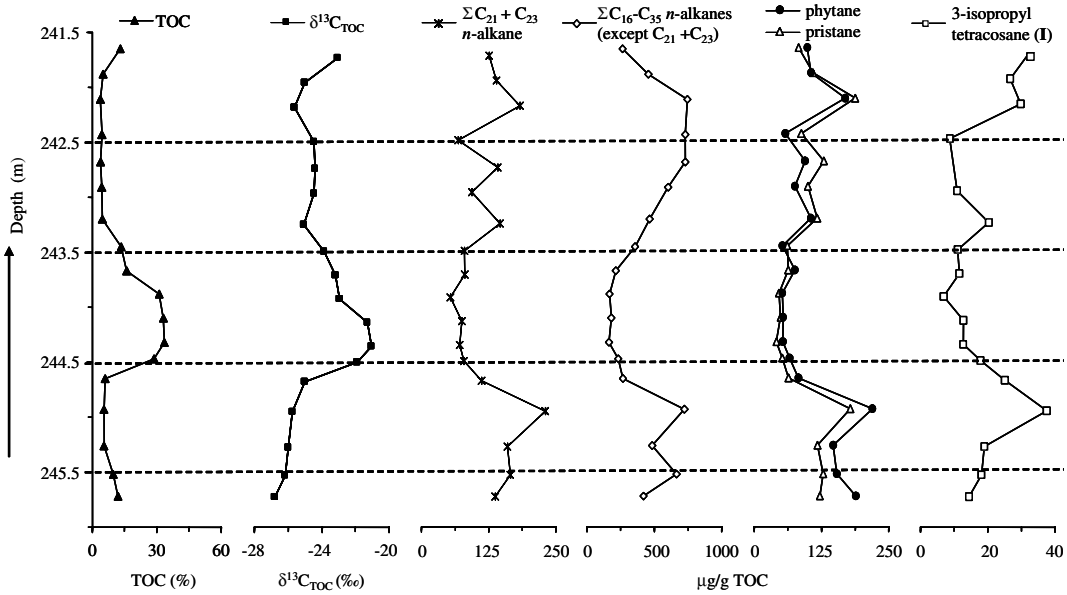

Fig. 2. TOC, $\delta^{13}C_{TOC}$ value and concentration (µg/g TOC) of C_{21} and C_{23} *n*-alkanes, summed C_{16}–C_{35} (excluding C_{21} and C_{23}) *n*-alkanes, phytane, pristane and 3-isopropyltetracosane (**I**) vs. depth.

exactly at peak TOC content. The *n*-alkane distribution showed distinct maxima at C_{21} and C_{23}, in agreement with previous reports (Fig. 3; e.g., Williams and Douglas, 1980, 1983; van Kaam-Peters et al., 1998). The $\delta^{13}C$ values of the *n*-alkanes showed the same pattern as reported by van Kaam-Peters et al. (1997, 1998), i.e. with substantially enriched values (2–16‰) for C_{23} and C_{21} over the C_{16}–C_{35} *n*-alkanes (Fig. 3). The $\delta^{13}C$ values of the weighted average of C_{21} and C_{23} *n*-alkanes varied from −17‰ to −25‰ and showed a similar depth trend as the $\delta^{13}C_{TOC}$ values, with maximum ^{13}C contents at the 243.5–244.5 m depth interval (Fig. 4). This trend was not observed, or was relatively small, for the $\delta^{13}C$ values of pristane, phytane, the other *n*-alkanes, or 3-isopropyltetracosane (**I**; Fig. 4). This latter component was the most ^{13}C-enriched saturated hydrocarbon biomarker, with $\delta^{13}C$ values of ca. −17‰.

3.2.2. Steroids and hopanoids

Concentrations of 5α-cholestane (**XVII**) and 4-methyl-5α-cholestane (**XVIII**) varied between 3 and 35 μg g^{-1} TOC and 4 and 17 μg g^{-1} TOC, respectively, with a minimum concentration at peak TOC values (Fig. 5). The distribution of hopanoids in the saturated hydrocarbon fractions was dominated by C_{29}–C_{30} neohop-(13)18-enes (**XXI**–**XXII**), (22*R*)-17α,21β(*H*)-homohopane (**XVII**) and 17α,21-β(*H*)-hopane (**XVIII**). The summed concentration of the two hopanes (**XIX**–**XX**) varied between 7 and 43 μg g^{-1} TOC and showed a concentration minimum at peak TOC values (Fig. 5). The summed concentration of the C_{29}–C_{30} neohop-(13)18-enes (**XXI**–**XXII**) varied between 10 and 76 μg g^{-1} TOC. In the aromatic hydrocarbon fractions substantial amounts of C_{25}–C_{26} aromatic hopanoids (**XXIII**–**XXIV**) were present and the summed concentration varied between 0.3 and 18 μg g^{-1} TOC. In contrast to the C_{30}–C_{31} hopanes (**XIX**–**XX**), a concentration maximum for the C_{25}–C_{26} aromatic hopanoids (**XXIII**–**XXIV**) was observed for this interval (Fig. 5).

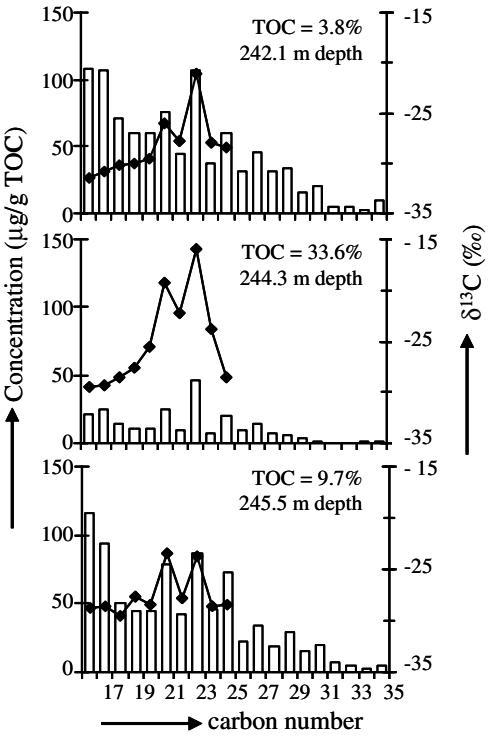

Fig. 3. Concentration (μg/g TOC) and $\delta^{13}C$ value (‰) of individual *n*-alkanes in saturated hydrocarbon fractions.

3.2.3. Derivatives of isorenieratene

The aromatic hydrocarbon fractions all contained abundant isorenieratene derivatives (**II**–**XVI**), as reported previously by van Kaam-Peters et al. (1997, 1998) and Sinninghe Damsté et al. (2001b). Internal distributions of the derivatives were similar in most of the sediments. In the majority the dominant components were **II**, **III**, **VI**, **VII** and **XV**. The summed concentrations of the isorenieratene derivatives (**II**–**XVI**) were highly variable, ranging from 35 to 410 μg g^{-1} TOC, with a maximum at peak TOC values (Fig. 5).

3.3. Kerogen

All flash pyrolysates of the kerogen were characterized by a series of *n*-alkanes and *n*-alkenes, alkylated thiophenes and benzothiophenes, and a series of alkyl benzenes (Fig. 6; cf. van Kaam-Peters et al., 1997, 1998; van Dongen et al., 2003b). Apart from discrete peaks, a large, S-rich UCM was present in all the kerogen pyrolysates (Fig. 6). Although the same compound classes were present in all the pyrolysates, their relative abundances differed substantially. The ratios of 2-methylthiophene to toluene, C_1–C_2 alkylated benzothiophenes to toluene and 2,3-dimethylthiophene to (1,2-dimethylbenzene + *n*-non-1-ene) changed substantially with depth (Fig. 7). All the ratios were higher in the peak TOC interval. In addition, the (2-ethylthiophene + 2,5-dimethylthiophene)/(2-ethylthiophene + 2,5-dimethylthiophene + 2,4 dimethylthiophene + 2,3-dimethylthiophene) ratio vs. depth showed sub-

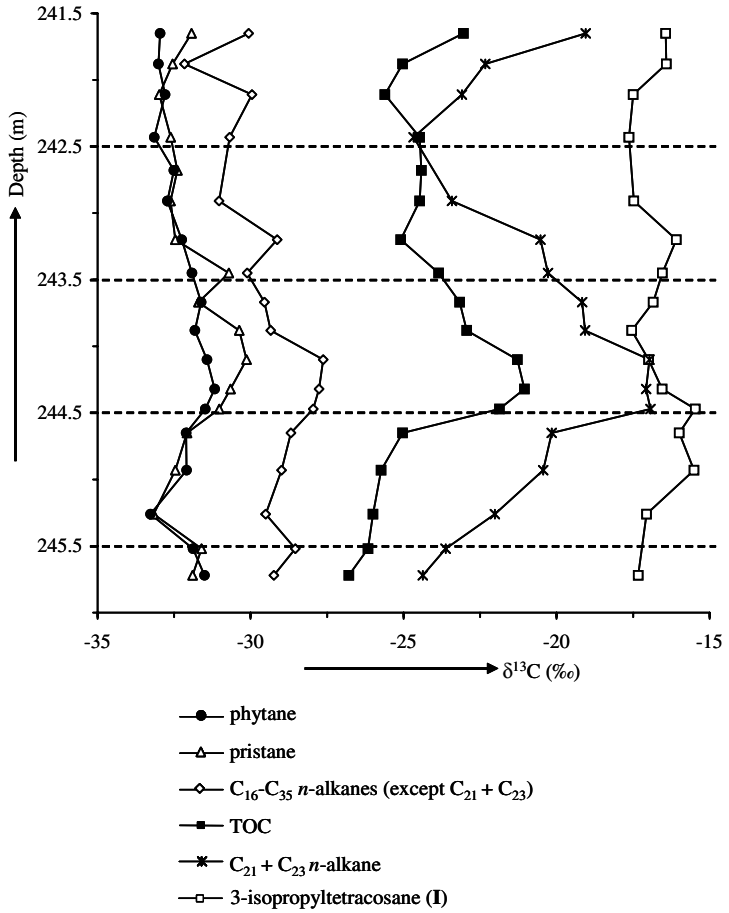

Fig. 4. The $\delta^{13}C$ value (‰) of 3-isopropyltetracosane (**I**), TOC, *n*-C_{21} and *n*-C_{23} *n*-alkanes, C_{16}–C_{35} (excluding C_{21} and C_{23}) *n*-alkanes, phytane and pristane vs. depth. For the *n*-alkanes, the $\delta^{13}C$ value of the weighted average is shown.

stantial changes (Fig. 7) and the highest values were found at peak TOC levels. The ratio of the UCM over C_{18}–C_{27} *n*-alkanes and *n*-alkenes also changed substantially with depth and showed higher values at peak TOC (Fig. 7).

4. Discussion

4.1. Organic carbon accumulation

The Blackstone Band section of the KCF is characterized by high (up to 34%) TOC levels (Table 1; Fig. 2). Such an enrichment can either be caused by an increase in the OC accumulation rate (OCAR) or by a decrease in the inorganic AR. A detailed age model is available for these Jurassic rocks through the recognition of obliquity (2–4 m wavelength) and precession cycles in three independent variables (Weedon et al., 2004). This allows determining OCAR if a constant sedimentation rate over the studied interval is assumed. However, such an assumption is likely not valid (cf. Weedon et al., 2004) since it would result in an up to five fold decreased flux of Al- and Si-containing minerals (which form a substantial part of the inorganic matrix of these sediments, Table 1) at the time of the peak TOC accumulation. In this situation, with high levels of TOC, it is more likely that an increased flux of OM resulted in a dilution of inorganic minerals and a temporary increase in the sedimentation rate. Therefore, another approach was used and TOC values were normalized to the Al content to correct for the dilution by inorganic minerals other than clay. This ratio can be used as a proxy for OCAR if the delivery of clay (the predominant source for Al) from the continents surrounding the basin remained constant over time. Like the TOC content (Fig. 2), the TOC/Al ratio

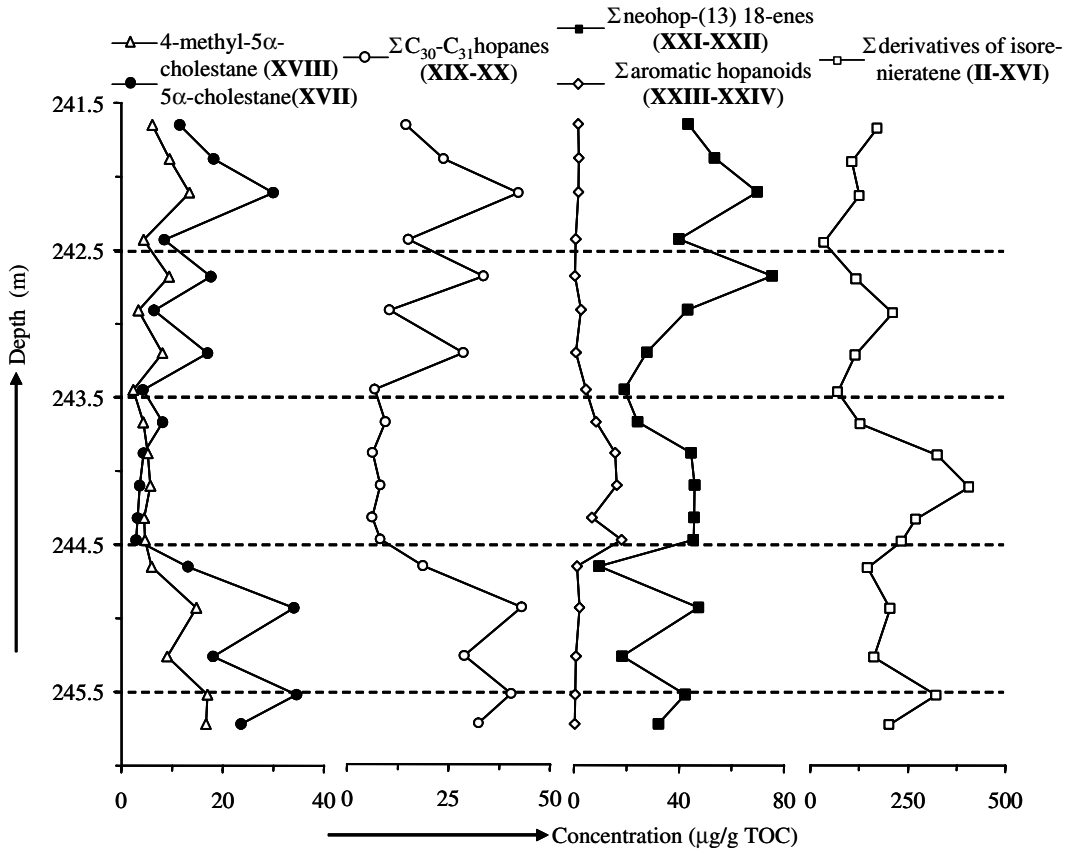

Fig. 5. Concentration (μg/g TOC) of hopanoids, steroids and isorenieratene derivatives (**II**–**XVI**) vs. depth.

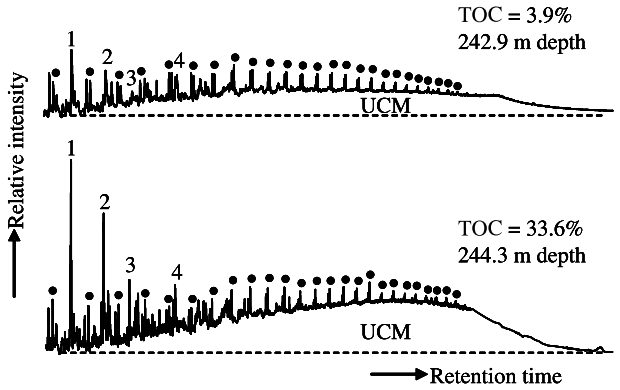

Fig. 6. Gas chromatograms of two typical kerogen flash pyrolysates of. Filled circles represent homologous series of *n*-alkanes/*n*-alkenes. 1 = 2-methylthiophene and toluene, 2 = 2,5-dimethylthiophene, *m*-xylene and *p*-xylene, 3 = 2-ethyl-5-methylthiophene and 4 = 1,2,3,4-tetramethylbenzene. Area between baseline and stippled line represents UCM.

(Fig. 8) shows a distinct maximum at 244.3 m depth. This maximum is even more distinct than in the TOC profile as the Al content in the TOC-rich interval drops substantially (Table 1). This suggests that the OCAR varied substantially.

This approach is strongly dependent on the assumption that the Al flux remains constant over time, which is probably not entirely realistic. It is, however, unlikely that the substantial increase in the TOC/Al ratio is completely due to a decrease

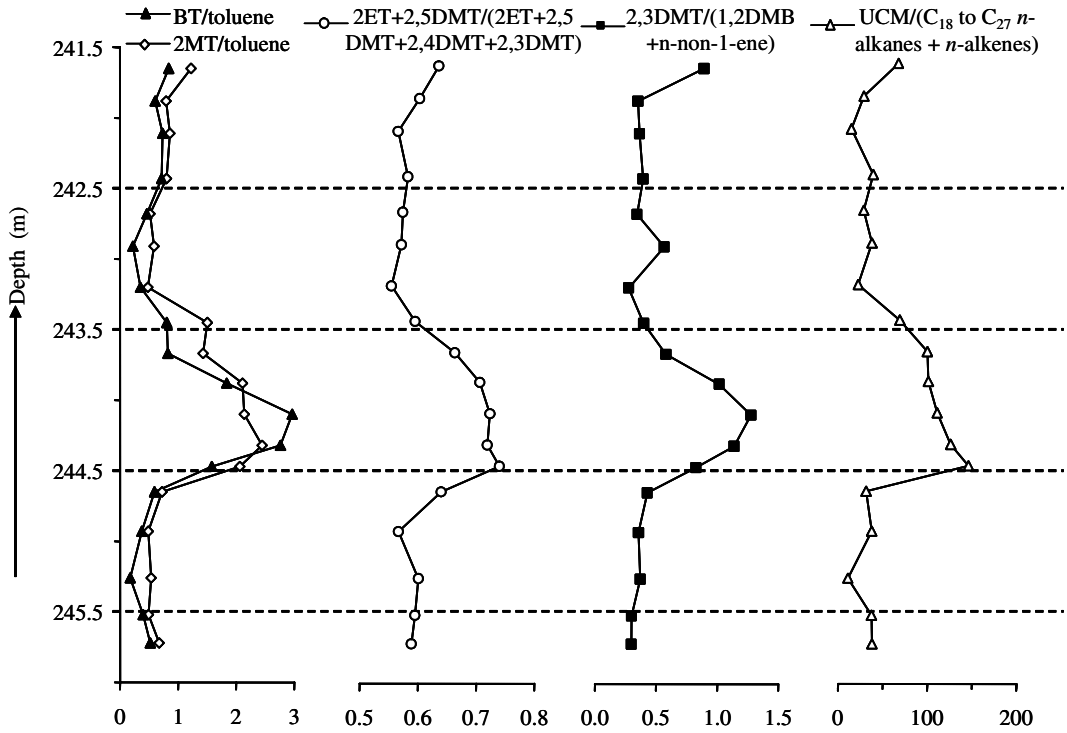

Fig. 7. Depth profiles of benzothiophenes over toluene, 2-methylthiophene over toluene, 2,3-dimethylthiophene over (1,2-dimethylbenzene + *n*-non-1-ene), 2-ethylthiophene + 2,5-diemethylthiophene over (2-ethylthiophene + 2,5-dimethylthiophene + 2,4-dimethylthiophene + 2,3-dimethylthiophene) and UCM/(C_{18} to C_{27} *n*-alkanes + *n*-alkenes) in kerogen pyrolysates. BT = benzothiophenes, MT = methylthiophene, DMT = dimethylthiophene, DMB = dimethylbenzene, ET = ethylthiophene.

in Al flux. If the Si/Al ratio is plotted vs. depth a distinct cyclicity is observed that is independent of the TOC cycle (Fig. 9) and likely related to variation in clay mineralogy, in particular the ratio of smectite to illite. The observed cycle (wavelength ca. 2.6 m) most likely reflects the strong obliquity cycle (38 ka) observed in the KCF (Weedon et al., 2004) and allows calculation of an average sedimentation rate of 6.8 cm ka^{-1}, in good agreement with the sedimentation rate of ca. 6 cm ka^{-1} reported for the complete *wheatleyensis* ammonite zone (Tyson, 2004). Ti is a tracer for dust input (Wehausen and Brumsack, 2000) and the Ti/Al ratio shows the same cyclicity as observed for Si/Al (Fig. 9). If we assume that the variation in these cycles is entirely due to variation in the Al flux, it has only varied by 25–30%. Moreover, both these ratios show minimum values at the time of the maximum in the TOC/Al ratio. Therefore, it is highly unlikely that only variation in the Al flux caused the distinct maximum in the TOC/Al ratio.

Based on the TOC/Al ratio profile the core-section can be divided in six different sub-sections (A–F in Fig. 8). Sub-section C has the highest TOC/Al values, sub-sections B and E the lowest values and sub-section D shows intermediate values. This indicates that these sections comprise one complete cycle, with sub-sections B and E corresponding to the start and the end of the cycle, respectively. The two remaining sub-sections, A and F, show slightly enhanced values in TOC/Al ratio compared to sub-sections B and E, and probably represent the start and end of two adjacent cycles. As these two sections are not part of the same Blackstone band TOC cycle they are not included in further discussions.

From the average TOC/Al ratios of the different sections (Table 2), an enrichment factor based on the average values of sub-section B and E relative to sub-section C can be calculated, showing that the TOC/Al ratio increases by a factor of 19 (Table 3). This suggests that an increase in OCAR was the primary cause of the increased TOC values in this single cycle. Assuming that the Al flux remained constant, the average sedimentation rate (6.8 cm ky^{-1} based on the observed obliquity cycle, Fig. 9) can

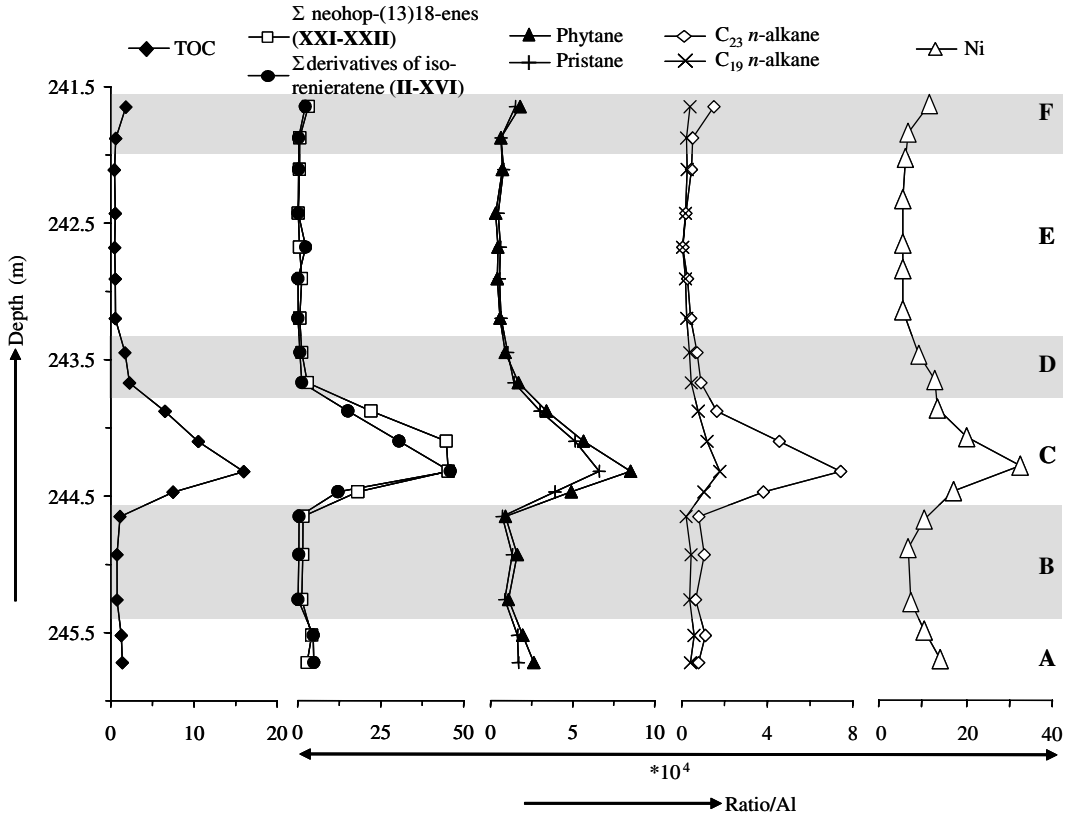

Fig. 8. Depth profiles of Al-normalized ratios of TOC, summed $C_{29} + C_{30}$ neohop-(13)18-enes (**XXI–XXII**), summed isorenieratene derivatives (**II–XVI**), phytane, pristane, C_{23} *n*-alkane and C_{19} *n*-alkane and Ni/Al ratio. Different sub-sections (defined in text) are separated by stippled lines and indicated with capital letters.

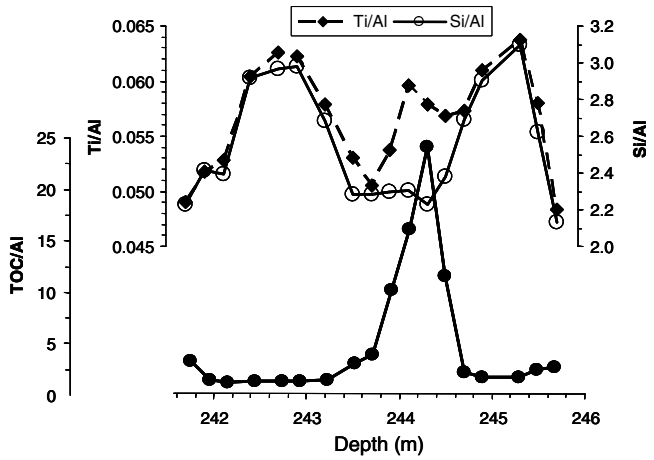

Fig. 9. Ti/Al, Si/Al and TOC/Al ratios vs. depth. The first two parameters show a distinct cyclicity independent of the TOC cycle.

be used, in combination with average Al concentrations, to calculate the sedimentation rate in each sub-section (Table 4). With these estimates, OCAR can be calculated assuming an average dry bulk density for organic material and inorganic material of 1.25 (Hartgers et al., 1995) and 2.7 g cm^{-3} (Kuhnt

Table 2
Average TOC/Al ratio and $\delta^{13}C$ value of TOC and biomarkers for sub-sections of Blackstone Band TOC cycle

Sub-section	TOC/Al ratio	TOC	$\delta^{13}C$ (‰) phytane	3-Isopropyl-tetracosane
B	0.9	−25.6	−32.5	−16.2
C	10.1	−21.8	−31.5	−16.6
D	2.0	−23.5	−31.8	−16.7
E	0.4	−24.8	−32.7	−16.8

Table 3
Enrichment of TOC and biomarkers in sub-section C relative to sub-sections B and E

Ratio (vs. Al)	Enrichment factor[a]
TOC	19
Pristane	7
Phytane	9
Σderivatives of isorenieratene (**II**–**XVI**)	41
ΣC_{30}–C_{31} hopanes (**XIX**–**XX**)	12
$\Sigma C_{29} + C_{30}$ neohop-(13)18-enes (**XXI**–**XXII**)	53
$\Sigma C_{25} + C_{26}$ aromatic hopanoids (**XXIII**–**XXIV**)	75
4-Methyl-5α-cholestanes (**XVIII**)	28
5α-Cholestane (**XVII**)	9
C_{21} *n*-alkane	10
C_{23} *n*-alkane	11
C_{19} *n*-alkane	6
3-Isopropyltetracosane (**I**)	11

[a] (average of sub-section C)/(average of sub-section B/E).

Table 4
Estimated sedimentation rate and OCAR in different sub-sections of KCF interval studied

Sub-section	Sedimentation rate (cm ky^{-1})	OCAR (gC m^{-2} y^{-1})
B	5.0	7.1
C	12.8	78
D	4.8	17
E	3.9	4.3

et al., 1990), respectively. The calculated OCARs (Table 4) vary from 4 gC m^{-2} y^{-1}in section E to 78 gC m^{-2} y^{-1} at the TOC peak (section C), an almost twenty fold increase. These values compare favourably with estimates of ca. 10 gC m^{-2} y^{-1} for average OCARs in complete ammonite biozones (Tyson, 2004) and for complete obliquity cycles (Weedon et al., 2004) in this part of the KCF. The high value of the Blackstone Band (78 gC m^{-2} y^{-1}) is remarkable but it should be realized that this is one of the beds richest in TOC in the KCF. High values of up to 58 gC m^{-2} y^{-1} for OCARs have been reported for present-day shelf sea settings (Tyson, 1995).

4.2. What is the cause of the large variation in $\delta^{13}C_{TOC}$?

Besides a cyclicity in TOC content, the Blackstone Band of the KCF is also characterized by relatively high $\delta^{13}C_{TOC}$ values (up to −21‰), also showing a cyclicity (Table 1; Fig. 2). When the TOC/Al ratios are plotted against the $\delta^{13}C_{TOC}$ values, the samples are distributed along two lines (Fig. 10). For sediments with a TOC/Al ratio <1.7, $\delta^{13}C_{TOC}$ seems to be independent of the TOC/Al ratio (line I in Fig. 10). However, for the OM-rich sediments (TOC/Al ratio >1.7, i.e. sediments with a TOC content >6%) there is a linear relationship between the TOC/Al ratio and $\delta^{13}C_{TOC}$ with higher $\delta^{13}C_{TOC}$ at higher TOC/Al ratios (line II in Fig. 10).

High $\delta^{13}C$ values can result from an enrichment in ^{13}C of the dissolved inorganic carbon ($\delta^{13}C_{DIC}$) in the palaeowater column or the phytoplankton carbon source, or from increased primary productivity, which may result in a decreased isotopic fractionation during photosynthesis (Laws et al., 1995; Popp et al., 1998). In both cases a similar shift as observed for the $\delta^{13}C_{TOC}$ would be expected for the $\delta^{13}C$ values of biomarkers derived from primary producers. As a general biomarker for primary producers, phytane, likely derived from the side chain of chlorophyll *a* in photoautotrophic organisms (Volkman and Maxwell, 1986), can be used. In contrast to the $\delta^{13}C_{TOC}$, the $\delta^{13}C$ value of phytane ($\delta^{13}C_{phytane}$) shows no substantial shift with increased TOC/Al ratio (Fig. 10). In addition, the $\delta^{13}C$ values for 3-isopropyltetracosane (**I**; $\delta^{13}C_{isoprop}$; Table 2), a biomarker with a very specific structure but of unknown marine origin (Schouten et al., 1998a), also remain constant with increasing TOC/Al values. This indicates that a shift in $\delta^{13}C_{DIC}$ of surface waters as well as a substantially increased primary production, resulting in reduced isotopic fractionation during photosynthesis, cannot be the primary cause for the observed shift in $\delta^{13}C_{TOC}$.

An alternative explanation could be that the changes in $\delta^{13}C_{TOC}$ at TOC/Al ratios >1.7 are caused by a mixing of marine and terrestrial OM. In present day systems terrestrial OM is relatively depleted in ^{13}C (between 4‰ and 12‰; Tyson, 1995) compared to marine OM. However, the difference between $\delta^{13}C$ values of terrestrial and marine OM in Jurassic times was quite different: terrestrial OM was not substantially depleted but slightly enriched in ^{13}C (Tyson, 1995). For instance, Jurassic

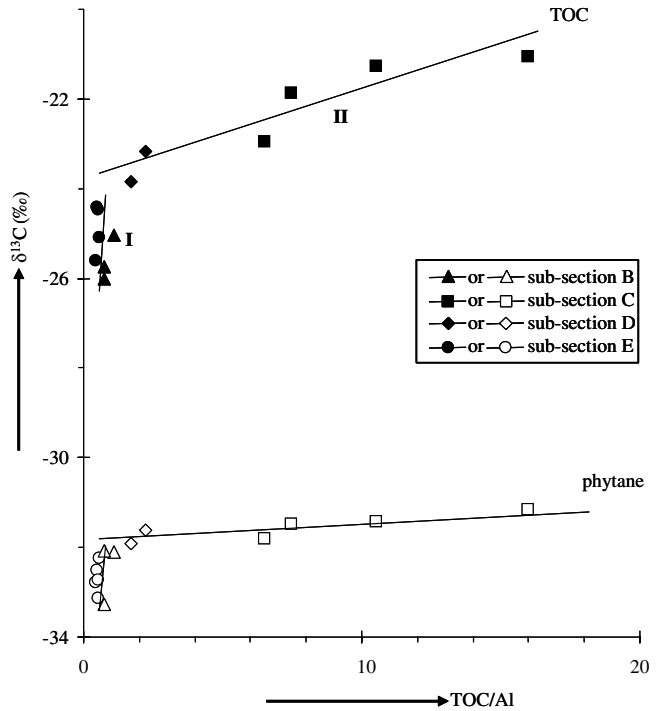

Fig. 10. Cross-plot of TOC/Al ratio and $\delta^{13}C_{TOC}$ (filled symbols) and $\delta^{13}C_{phytane}$ (open symbols) value. Lines I and II are linear regression lines through samples from sub-sections B and E and C and D, respectively. Sub-sections defined as in Fig. 8.

wood has $\delta^{13}C$ values around $-25‰$ (Hesselbo et al., 2000, 2002). This value is approximately 3‰ enriched relative to the estimated $\delta^{13}C$ value around $-28‰$ of Jurassic marine OM, derived from $\delta^{13}C_{phytane}$ and the typical 4‰ offset between $\delta^{13}C_{phytane}$ and $\delta^{13}C_{TOC}$ (Collister et al., 1992; Schouten et al., 1998b). This indicates that the differences in $\delta^{13}C$ values between terrestrial and marine derived material are relatively small and cannot account for the observed shifts in $\delta^{13}C_{TOC}$. In addition, analysis of kerogen pyrolysates of all samples showed only minor contributions of compounds of terrestrial origin (Fig. 6). These observations are confirmed by microscopic observations of comparable KCF sediments, which also reveal a low contribution of terrestrial OM (e.g., Huc et al., 1992; Boussafir et al., 1995; van Kaam-Peters et al., 1998; Tyson, 1989). This indicates that the observed 3–4‰ enrichment in $\delta^{13}C_{TOC}$ in sub-section C (Table 2) must be due to variation in the marine component of the sedimentary OM and is not the result of varying contributions of terrestrially-derived OM.

The changes in $\delta^{13}C_{TOC}$ value can potentially be caused by a shift in the relative contribution of marine sources with different isotopic compositions. Specifically, an increased contribution of an isotopically enriched source in the TOC-rich part of the TOC cycle would then be expected. A large range of $\delta^{13}C$ values is apparent for the marine biomarkers in the KCF, with two distinct ^{13}C enriched sources. The first group of ^{13}C-enriched biomarkers are the derivatives of isorenieratene (**II**–**XVI**), originating from Chlorobiaceae (green sulfur bacteria; Koopmans et al., 1996) with $\delta^{13}C$ values of ca. $-17‰$ (van Kaam-Peters et al., 1997, 1998). Their enriched $\delta^{13}C$ values result from the distinct biochemical inorganic carbon fixation pathway of Chlorobiaceae, i.e. the reversed tricarboxylic acic cycle (Sirevåg and Ormerod, 1970; Summons and Powell, 1986; Sinninghe Damsté et al., 1993b; van der Meer et al., 1998; van Breugel et al., 2005). Another ^{13}C-enriched biomarker is 3-isopropyltetracosane (**I**), also with $\delta^{13}C$ values around $-17‰$ (Fig. 4). It originates from an unidentified marine organism (Schouten et al., 1998a). In addition, enriched $\delta^{13}C$ values for the C_{21} and C_{23} *n*-alkanes were also observed, with the most ^{13}C-enriched values at peak TOC (Fig. 4). Schouten et al. (1998a) postulated on biochemical and isotopic grounds

that these *n*-alkanes also derive from the unknown marine organism responsible for the 3-isopropyltetracosane (**I**). Consequently, the *n*-alkanes from this source would have $\delta^{13}C$ values around −17‰. Both *n*-alkanes as well as the other *n*-alkanes would also originate from photoautotrophs with $\delta^{13}C$ values around −30‰. A mixed input from both sources is thus the most likely explanation for the observed shifts (Fig. 4).

An enhanced contribution of cell material from these ^{13}C-enriched marine organisms could explain the enrichment in $\delta^{13}C_{TOC}$ values. If this were the case, an enhanced input of their biomarkers would be expected. To verify this, the enrichment factors for the ratios of the individual biomarkers over Al (Fig. 8) were determined in an identical way as described for the TOC/Al enrichment factor (Table 3). These enrichment factors were compared with the enrichment factor for TOC as well as for phytane, a general biomarker for non ^{13}C-enriched photoautotrophs. The 3-isopropyltetracosane (**I**), as well as the C_{21} and C_{23} *n*-alkanes, shows enrichment factors which are a factor 2 lower than that of TOC but comparable to that of phytane (Table 3). This suggests that the contribution to biomass from the unidentified organism responsible for these relatively ^{13}C-enriched biomarkers remains relatively constant compared to the input of photoautotrophic OM and so cannot be responsible for the shift in $\delta^{13}C_{TOC}$. In contrast, the enrichment factor for isorenieratene derivatives (**II**–**XVI**) was approximately 4–5 times higher than for phytane and ca. 2 times higher than for TOC (Table 3), suggesting that an increased contribution of biomass originating from Chlorobiaceae could cause the enrichment in ^{13}C of TOC. In that case, large amounts of cell material from Chlorobiaceae would be preserved and this should be revealed by the composition of the kerogen pyrolysates. Hartgers et al. (1994a,b) showed that kerogen pyrolysates of sediments anomalously enriched in derivatives of diaromatic carotenoids contain 1,2,3,4-tetramethylbenzene (TMB) as the dominant constituent. This product is formed by thermal breakdown of macromolecularly-bound diaromatic carotenoids in the kerogen. However, isotopic considerations indicated that even those sediments contain no other preserved biomass from these green sulfur bacteria (Hartgers et al., 1994a). In the KCF sediments the abundance of TMB in the kerogen pyrolysates is substantially smaller than in the sediments studied by Hartgers et al. (1994a); Fig. 6. This suggests that preservation of large amounts of biomass of Chlorobiaceae did not occur and indicates that it is unlikely that preservation of ^{13}C-enriched biomass from marine OM with an enriched $\delta^{13}C$ signature is the primary cause for the shift in $\delta^{13}C_{TOC}$.

Since a shift in marine sources seems not to be the origin of the observed shift in $\delta^{13}C_{TOC}$ values, it is possible that it was caused by a change in the relative preservation of different, isotopically distinct, compound classes. Clues for such a shift are obtained from the flash pyrolysates of the kerogen (Fig. 6), which reveal a marked change in composition with increasing TOC/Al ratio. Specifically, the relative contribution of OSCs, i.e. the short-chain alkylated thiophenes and benzothiophenes and the S-rich UCM, substantially increase in sediments with TOC/Al >1.7 (Fig. 11). The summed OSCs and the S-rich UCM can make up the major fraction of the GC-amenable part of the kerogen pyrolysate and, thus, the OM. It was shown that the short chain alkylated thiophenes as well as the S-rich UCM in pyrolysates of KCF kerogen were relatively enriched in ^{13}C compared to the lipid derived OC (van Kaam-Peters et al., 1998; van Dongen et al., 2003b). This suggests that a relative increase in the contribution of their precursors to the kerogen would cause a substantial enrichment in the $\delta^{13}C_{TOC}$ value. It has been shown that these short chain alkylated thiophenes (as well as the S-rich UCM) originate from carbohydrates, which became incorporated into kerogen during early diagenesis by reaction with reduced inorganic species (i.e. sulfurization) instead of being remineralized (van Kaam-Peters et al., 1998; Sinninghe Damsté et al., 1998; van Dongen et al., 2003a,b). Kok et al. (2000b) showed that laboratory sulfurization of fresh algal biomass resulted in the formation of sulfurized material that, upon pyrolysis, yielded alkylated thiophenes and an S-rich UCM and concomitantly showed a drop in the yield of hydrolysable carbohydrate monomers from 35 to 14 wt%. Carbohydrates can be substantially enriched in ^{13}C, up to 16‰, compared with lipids within single organisms (Sinninghe Damsté et al., 2001b; van Dongen et al., 2002); this explains the ^{13}C-enriched $\delta^{13}C$ values for the short chain alkylated thiophenes and the S-rich UCM (van Kaam-Peters et al., 1998; van Dongen et al., 2003b). Thus, the more ^{13}C-enriched $\delta^{13}C_{TOC}$ values at peak TOC/Al values (Fig. 10) can be explained by an increased contribution of sulfurized carbohydrate carbon.

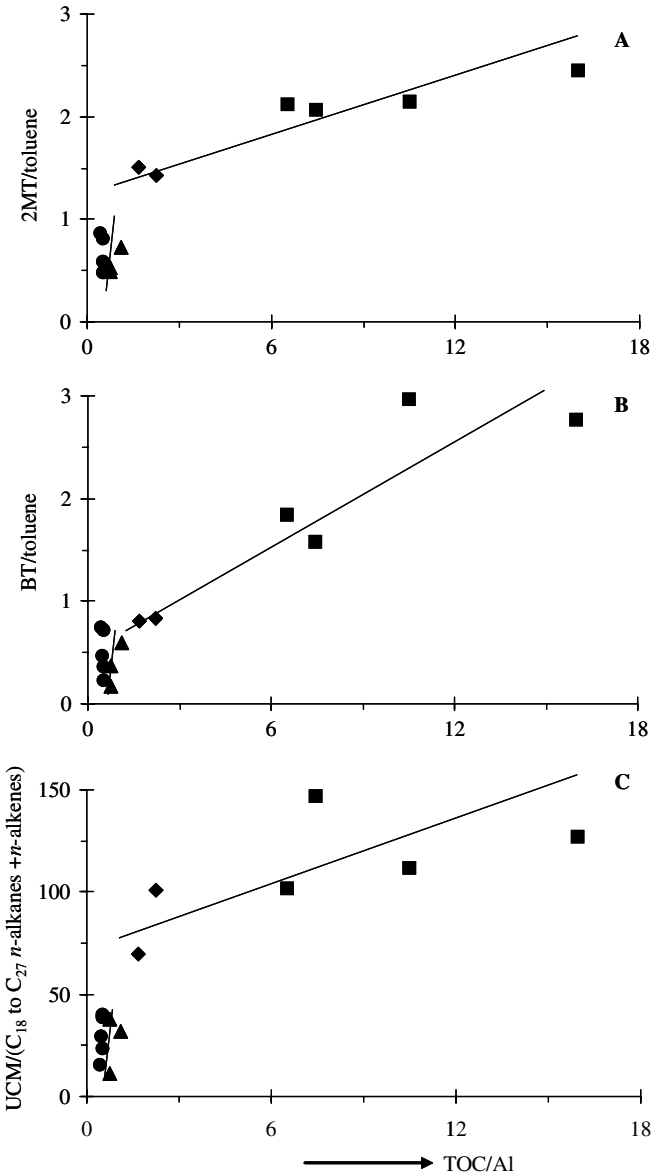

Fig. 11. Cross-plot of TOC/Al ratio and ratio of (A) 2-methylthiophene over toluene, (B) benzothiophenes over toluene and (C) UCM/(C_{18} to C_{27} *n*-alkanes + *n*-alkenes) in KCF kerogen pyrolysates. MT = methylthiophene, BT = benzothiophene. Symbols represent subsections and are defined in Fig. 10. The benzothiophenes quantified are the six most abundant C_1 alkylated benzothiophene isomers.

Carbohydrates, which may form a large part (up to 70%) of the OM produced during photosynthesis by primary producers in the upper part of the water column (Romankevich, 1978; Benner et al., 1992; Pakulski and Benner, 1992; Skoog and Benner, 1997), are generally rapidly mineralized to a large degree under oxic (e.g., Hernes et al., 1996; Hedges et al., 1999) and even under anoxic conditions (Arnosti et al., 1994; Arnosti and Repeta, 1994; Arnosti, 1995). However, if, for some reason, carbohydrates could be preserved to a high degree, this would not only cause an enrichment in $\delta^{13}C_{TOC}$ value but also result in a substantial increase in OCAR. The varying degree in relative preservation of carbohydrates could thus explain the observed relationship between $\delta^{13}C_{TOC}$ values and TOC/Al ratios (Fig. 10; line II), while primary production rates remained more or less constant as suggested

by the almost constant $\delta^{13}C$ values of algal biomarkers (Fig. 4; Table 2). This does not, however, exclude the possibility that a small increase in primary production could have triggered a much increased preservation of OM through the creation of a higher oxygen demand in the water column, resulting in anoxia.

4.3. Relative preservation of lipid and carbohydrate carbon

Because on average only 5% of the total carbon in the OM of marine primary producers is present as lipid material (Romankevich, 1978), the large increase in OCAR estimated for sub-section C (i.e. up to almost 80 $gC\,m^{-2}\,y^{-1}$, Table 4), in combination with the relatively minor changes in primary production, could not have been caused only by the preservation of diagenetically resistant lipid material (e.g., lipid biopolymers; for a review see de Leeuw and Largeau, 1993) but 'labile' cell material, like carbohydrates or proteins, must also be involved. In contrast to the evidence for the preservation of carbohydrate carbon (see above), no indications at the molecular level were obtained for preservation of OM derived from proteins. The C/N ratios for the kerogen and UCM in the kerogen pyrolysate of the Blackstone Band are 40 and 98, respectively (van Dongen et al., 2003b) and, thus, also do not seem to point to an important contribution of proteins, which would require lower C/N ratios. It should be noted, however, that for some other ancient sediments indications exist for preservation of labile OM derived from proteins (Riboulleau et al., 2002) and that this material would likely also be ^{13}C-enriched relative to the lipid fraction. Therefore, in the following discussion we refer to this labile carbon pool as "carbohydrate carbon" but we do not fully exclude some contribution from proteins.

In order to estimate the increase in preservation of lipid and carbohydrate carbon, the proportion of these two different carbon pools to the TOC was calculated. Assuming that lipid and carbohydrate carbon are the main contributors to the sedimentary OM, the contribution of both carbon pools to the TOC was calculated using the $\delta^{13}C_{TOC}$ and a two end member mixing model, consisting of the $\delta^{13}C$ of lipid carbon ($\delta^{13}C_{lipid}$) and the $\delta^{13}C$ value of carbohydrate carbon ($\delta^{13}C_{carbohydrate}$). For $\delta^{13}C_{lipid}$ a value of $-28‰$ is inferred, based on an average $\delta^{13}C$ value of lipid carbon measured on *n*-alkanes and *n*-alkenes in the kerogen pyrolysates (van Kaam-Peters et al., 1998). The $\delta^{13}C_{carbohydrate}$ is estimated by assuming a difference in $\delta^{13}C$ value between $\delta^{13}C_{lipid}$ and $\delta^{13}C_{carbohydrate}$ of $7 \pm 2‰$. The 7‰ estimate is the most realistic since it is the average difference observed between lipids and carbohydrates within single organisms (Sinninghe Damsté et al., 2001b; van Dongen et al., 2002). Using the average $\delta^{13}C_{TOC}$ value of the sub-sections (Table 2), the proportions of lipid- and carbohydrate-derived carbon in sub-sections B and E (using an average) and sub-section C were calculated. In sub-section C, the calculation shows that a substantial part (up to almost 90%) of the OC originates from carbohydrate carbon (Table 5), depending on the assumed value for $\delta^{13}C_{carbohydrate}$. For sub-sections B and E with reduced TOC content, a substantial part (31–76%) of the OC may still originate from carbohydrate carbon, with a roughly equal part (24–69%) originating from lipid carbon (Table 5). The relatively high proportion of carbohydrate carbon in sections B/E may seem surprising but it should be realized that these sections still have high TOC values (>4%) and were deposited under anoxic conditions. In addition, kerogen pyrolysates from sections B and E reveal the presence of substantial amounts of short chain alkylated thiophenes as well as an S-rich UCM, thereby also pointing to a substantial contribution of carbohydrate carbon.

On average, approximately 40% of the total OM of a marine primary producer is present as carbohydrate and only 5% as lipid (Romankevich, 1978), i.e. carbohydrates are a factor 8 more abundant than lipids. With the calculated proportion of carbohydrate and lipid carbon, this ratio was calculated for sections B/E and C for the different assumptions with respect to $\delta^{13}C_{carbohydrate}$ (Table 5). This shows, for the most realistic assumption for $\delta^{13}C_{carbohydrate}$ (i.e. $-21‰$), that in the TOC-leanest section the ratio is 0.7, i.e. lipids are a factor >10 better preserved than carbohydrates. In strong contrast, the value is 7.7 for the TOC-rich section, indicating almost no selective preservation of lipids relative to carbohydrates. This latter value is strongly dependent on the assumed $\delta^{13}C_{carbohydrate}$; for $\delta^{13}C_{carbohydrate} = -19‰$ it drops to 2.2 (Table 5). These calculations indicate that a substantial increase in the preservation of carbohydrate carbon can explain the shift in $\delta^{13}C_{TOC}$ and at the same time result in substantially increased OM burial

Table 5
Calculated proportion of lipid and carbohydrate carbon in sub-sections B/E and C for different assumed $\delta^{13}C_{carbohydrate}$ values and resulting carbohydrate C/lipid C ratio

Sub-section	B/E[a]	C	B/E[a]	C	B/E[a]	C
$\delta^{13}C_{carbohydrate}$ (‰):	−23		−21		−19	
Proportion of lipid carbon	0.24	Na[b]	0.60	0.11	0.69	0.31
Proportion of carbohydrate carbon	0.76	Na[b]	0.40	0.89	0.31	0.69
Carbohydrate C/lipid C	1.3	Na[b]	0.7	7.7	0.5	2.2

[a] Average of sub-section B and E.
[b] Na = not applicable because isotopic difference between carbohydrate and lipid carbon not large enough to allow to calculation.

flux, without the need to substantially increase primary productivity.

4.4. What caused the enhanced carbohydrate preservation?

Our data seem to indicate that the KCF Blackstone Band TOC cycle can be explained by a substantial increase in OCAR (Table 4) through a substantial increase in the preservation of carbohydrates. This can be visualized in a theoretical model in which three depositional stages can be distinguished (Fig. 12). In the first (Fig. 12A) there are no anoxic bottom waters and sedimentary pore waters are oxic in the surface sediment. Under these conditions [i.e. a long oxygen exposure time (OET) – the time that OM is exposed to oxygen in both the water column and sediment (Hartnett et al., 1998)] by far the largest fraction of the carbohydrates produced in the upper water column would be mineralized and mineralization could continue in the anoxic part of the sediment (Arnosti, 1995; Arnosti et al., 1998). In the second stage of the model (Fig. 12B), there is bottom water euxinia, resulting in substantially reduced OET for settling OM. This, in combination with the relatively shallow water column (only ca. 75 m; Weedon et al., 2004), results in the delivery of substantially increased amounts of carbohydrate material at the sediment/water interface, although most of the carbohydrate is still probably mineralized during transport through the predominantly oxic water column (Hernes et al., 1996). Recent work has demonstrated, however, that anoxic conditions considerably decrease and even shut down the breakdown of labile OM, including carbohydrates (Moodley et al., 2005). The enhanced euxinic conditions would thus allow the carbohydrates that do reach the sediment/water interface to become sulfurized through reaction

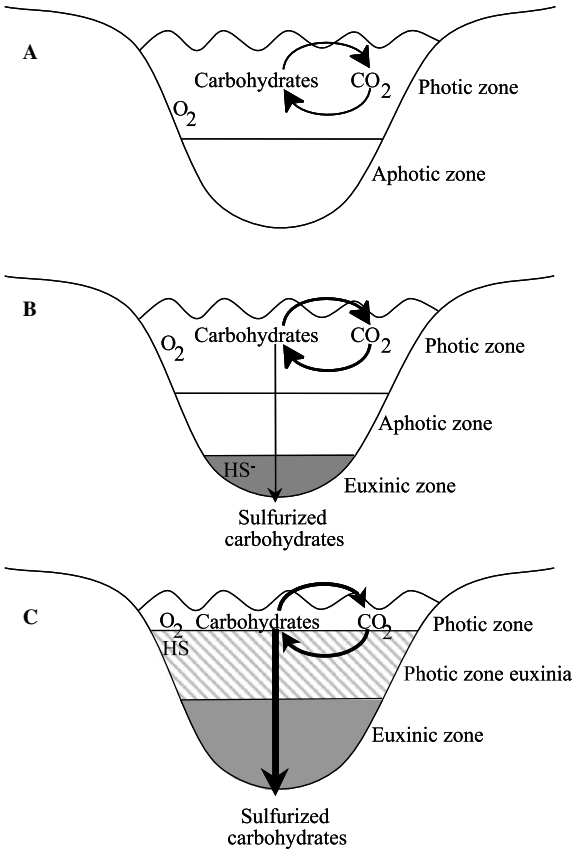

Fig. 12. Depositional model, illustrating influence of anoxic depositional conditions on preservation of carbohydrate carbon. (A) Stage 1: Oxic conditions in water column and oxic pore waters in surface sediment; no preservation of carbohydrates through sulfurization. (B) Stage 2: Euxinic conditions in bottom waters; increased preservation of carbohydrate through sulfurization. (C) Stage 3: photic zone euxinia; relatively great preservation of carbohydrate through sulfurization.

with reduced inorganic sulfur species during early diagenesis (Kok et al., 2000b; van Dongen et al., 2003a). Sulfurization of OM is a relatively slow process that takes hundreds to thousands of years

to be completed (Werne et al., 2000; Kok et al., 2000a; Sinninghe Damsté et al., 2006) but the substantially reduced mineralization of carbohydrates under anaerobic conditions would allow a substantial fraction of the carbohydrate to become sulfurized. When carbohydrate becomes sulfurized, anaerobic bacteria are probably no longer able to use it as a source of carbon and energy, although this remains to be experimentally verified. Sulfurization of carbohydrates is therefore likely to result in preservation rather than mineralization of carbohydrate carbon. In the third stage of the model (Fig. 12C) euxinic conditions extend into the photic zone of the water column, resulting in photic zone euxinia (PZE). These conditions further decrease the OET of settling OM, resulting in a substantially greater fraction of carbohydrate carbon reaching the sediment floor and being available for sulfurization.

In the sediments of the Blackstone Band cycle, substantial amounts of the derivatives of isorenieratene (**II**–**XVI**) are present (Fig. 5). These biomarkers reveal the presence of green sulfur bacteria, which require both light and sulfide, and so provide evidence that PZE occurred (Sinninghe Damsté et al., 1993b; Hartgers et al., 1994b; Koopmans et al., 1996). In addition, substantial amounts of C_{29}–C_{30} neohop-13(18)-enes (**XXI**–**XXII**) and C_{25}–C_{26} aromatic hopanoids (**XXIII**–**XXIV**) were present (Fig. 5), possibly originating from bacteria dwelling at or below the chemocline, again pointing to a more stratified water column (Sinninghe Damsté, 1997). The presence of these PZE indicators throughout the section indicates that the third stage of the model was common. However, the ratios of the summed concentration of the derivatives of isorenieratene (**II**–**XVI**)/Al, the C_{29}–C_{30} neohop-13(18)-enes (**XXI**–**XXII**)/Al and the C_{25}–C_{26} aromatic hopanoids (**XXIII**–**XXIV**)/Al, all have a distinct maximum coinciding with peak TOC/Al ratios (Fig. 8). In addition, the enrichment factors were substantially higher than the phytane/Al ratio (Table 3). This indicates that, during deposition of the Blackstone Band the occurrence of PZE (the third stage in the model; Fig. 12) was more frequent or that the PZE periods lasted longer than those represented by the under- and overlying strata. This is confirmed by the substantially increased levels of trace elements (Co, Cr, Cu, Ni and V) normalized against Al levels which occur in section C along with peak TOC values (e.g., Ni/Al ratio in Fig. 8). Scavenging of these elements is optimal when the water column is anoxic (cf. Nijenhuis et al., 1999).

Consequently, during the whole TOC cycle alternations between the second and third stage occurred, but the duration of the third stage during deposition of sediment with a lower TOC/Al ratio was relatively shorter. These alternations may even have occurred on a seasonal basis (cf. Kenig et al., 2004). The longer duration of the third stage during deposition of the Blackstone Band most likely caused the preservation of more carbohydrate carbon through sulfurization and thus resulted in enhanced TOC values and ^{13}C-enrichment of the OM (line II in Fig. 10).

In contrast to the Blackstone Band, Morgans-Bell et al. (2001) showed that under- and overlying strata are less laminated and are in some places bioturbated. This probably indicates that occasional short-lived oxygenation events occurred in these sections. Such oxygenation events would substantially increase the OET of the deposited OM, which in turn could reduce the relative amount of preserved carbohydrate, causing a shift in $\delta^{13}C_{TOC}$ towards lower values. This could potentially be an explanation for the observed shifts in $\delta^{13}C_{TOC}$ values for TOC/Al <1.7 (line I in Fig. 10). In addition, such oxygenation events would also lower the Rock-Eval hydrogen index, which is reduced substantially at lower TOC contents in the KCF (e.g., Huc et al., 1992).

The occurrence of PZE can be caused by a climatically-induced increase in primary productivity, for instance by a slight increase in the run-off from the mainland, supplying more nutrients to the basin. This would cause a slightly enhanced productivity and consequently a higher oxygen demand in the water column. This higher oxygen demand would result in a shallowing of the chemocline which would minimize the OET. This would cause an increase in the amount of carbohydrates that reaches the sediment/water interface, resulting in optimal conditions for the preservation of carbohydrate carbon through sulfurization, TOC accumulation and ^{13}C-enrichment of OM. Another possibility is that the chemocline shifted to shallower depths due to changes in the physical conditions in the water column, for instance by an increased influx of denser or colder water. Such water masses would push up the original bottom water, causing a shallowing of the chemocline. In this way, nutrients "locked" below the chemocline would be advected to the photic zone, resulting in enhanced primary

productivity. In addition, a shift in the chemocline would minimize the OET, causing an increase in the amount of OM that reached the sediment/water interface, resulting in optimal conditions for preservation of carbohydrate through sulfurization and consequently enhanced TOC values and ^{13}C-enrichment of OM.

4.5. Implications for the KCF and other sedimentary environments

Although the TOC cycle comprising the Blackstone Band is the cycle in the KCF which reaches the highest TOC content, there are numerous other TOC cycles in the KCF that are characterized by substantially enhanced $\delta^{13}C_{TOC}$ values (Morgans-Bell et al., 2001). Huc et al. (1992) and van Kaam-Peters et al. (1998) also observed a significant correlation between TOC and $\delta^{13}C_{TOC}$ for a set of sediments covering a stratigraphically greater part of the KCF. In sediments deposited in other TOC cycles, substantial amounts of PZE markers as well as high amounts of preserved carbohydrate carbon (short chain alkylated thiophenes and S-rich UCM) have also been observed (van Kaam-Peters et al., 1998). In addition, Boussafir et al. (1995) concluded, on the basis of transmission electron microscopic observations, that OM sulfurization played an important role in another TOC cycle. Pancost et al. (2005) also reported, for the lower *hudlestoni* ammonite biozone of the KCF, a strong correlation between TOC content and the abundance of the sulfur-rich UCM in kerogen pyrolysates. Thus, the process proposed here for the TOC cycle comprising the Blackstone Band most likely played an important role in intervals throughout the KCF, albeit not as extreme as in the Blackstone Band. This suggests that the preservation of carbohydrates through sulfurization could exert an important primary control on the TOC cyclicity in the KCF.

Short chain alkylated thiophenes and an S-rich UCM have been commonly observed in other kerogen pyrolysates, especially from shallow, sedimentary environments (e.g., Sinninghe Damsté and de Leeuw, 1992; Sinninghe Damsté et al., 1992, 1993a, 1999; Hartgers et al., 1995; van Kaam-Peters and Sinninghe Damsté, 1997; Mongenot et al., 1999; Riboulleau et al., 2000, 2003). In addition, substantial changes in $\delta^{13}C_{TOC}$ are commonly observed without a concurrent shift in $\delta^{13}C$ value of the biomarkers from primary producers, for instance in the Peterborough Member of the Oxford Clay (Kenig et al., 1994). In these cases, it is also likely that carbohydrate carbon preservation through sulfurization played an important role in the accumulation of TOC, especially in the case of elevated organic S content. Thus, the process could play a much more important role in the preservation of OC than recognized till now, especially in shallow euxinic shelf seas.

5. Conclusions

The enhanced TOC contents in the Blackstone Band cycle of the KCF are probably caused by an increase in the OCAR and not by a decrease in the accumulation rates of inorganic matter. The calculated relative preservation factors suggest that enhanced preservation of carbohydrates through sulfurization, and not an increase in primary production, exerts the primary control on OCAR and $\delta^{13}C_{TOC}$ values in this TOC cycle. The enhanced preservation is most likely caused by a longer duration of photic zone euxinia in the depositional environment, conditions which foster the preservation of labile carbohydrate carbon through minimal oxygen exposure times and optimal conditions for sulfurization of OM. Enhanced preservation of carbohydrate carbon through sulfurization is probably a dominant control for OC accumulation in the KCF and could play a more important role than recognized till now in the preservation of OC in marine sediments, especially in shallow euxinic shelf seas.

Acknowledgements

We thank M. Kienhuis, E. Panoto and G. Nobbe for analytical assistance. Dr. S. Turgeon (University of Oldenburg) is thanked for providing the XRF measurements. The 'Anatomy of a Source Rock' project of The Natural Environment Research Council's Rapid Global Geological Events (RGGE) is thanked for the opportunity to collect samples from the Swanworth Quarry 1 core. Dr. J. Marshall (Southampton Oceanography Centre) is thanked for assistance during sampling, Dr. H. Morgans-Bell (University of Oxford) for the log data and A. Forster and Dr. J. Werne for helpful discussions. We thank Dr. N. Tribovillard and four anonymous referees for constructive criticism. The research was financially supported by the Netherlands-Bremen Oceanography Program (NEBROC).

Appendix

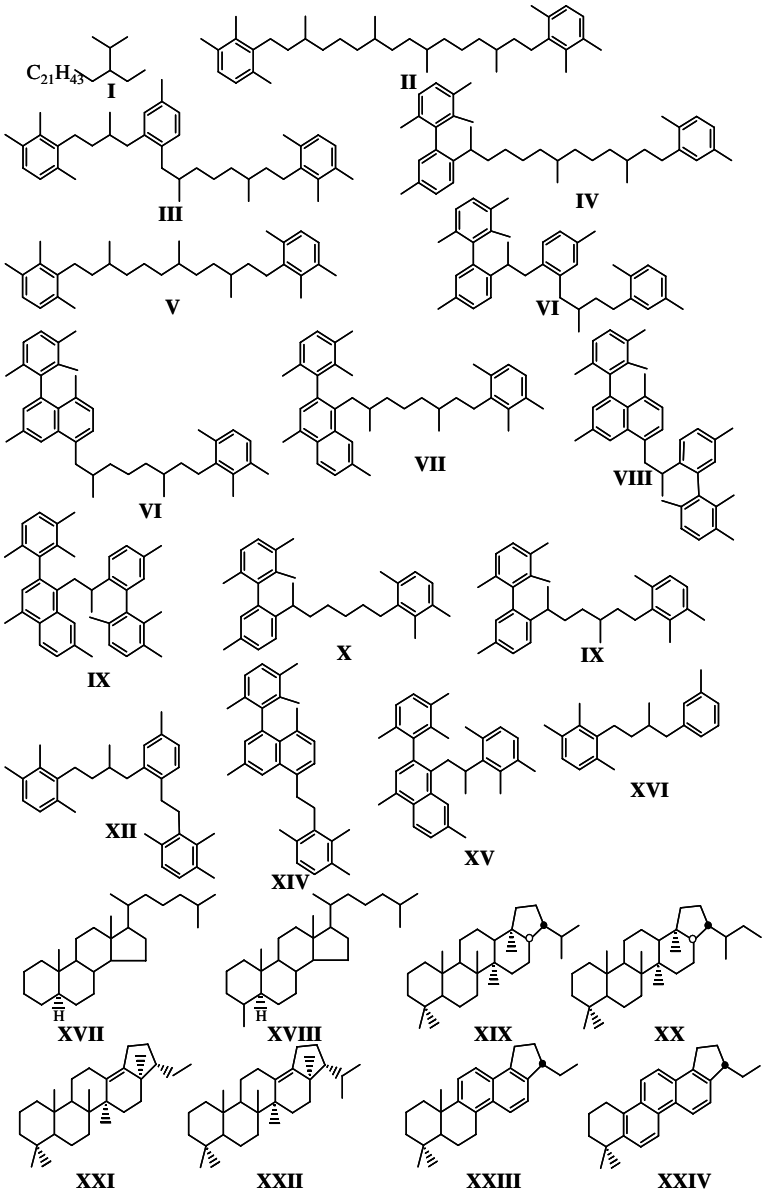

Associate Editor—**J.R. Maxwell**

References

Arnosti, C., 1995. Measurement of depth- and site-related differences in polysaccharide hydrolysis rates in marine sediments. Geochimica et Cosmochimica Acta 59, 4247–4257.

Arnosti, C., Jørgensen, B.B., Sagemann, J., Thamdrup, B., 1998. Temperature dependence of microbial degradation of organic matter in marine sediments: polysaccharide hydrolysis, oxygen consumption, and sulfate reduction. Marine Ecology Progress Series 165, 59–70.

Arnosti, C., Repeta, D., 1994. Oligosaccharide degradation by anaerobic marine bacteria: characterization of an experimental system to study polymer degradation in sediments. Limnology and Oceanography 39, 1865–1877.

Arnosti, C., Repeta, D.J., Blough, N.V., 1994. Rapid bacterial degradation of polysaccharides in anoxic marine systems. Geochimica et Cosmochimica Acta 58, 2639–2652.

Benner, R., Pakulski, J.D., McCarthy, M., Hedges, J.I., Hatcher, P.G., 1992. Bulk chemical characteristics of dissolved organic matter in the ocean. Science 255, 1561–1564.

Bertrand, P., Lallier-Vergès, E., 1993. Past sedimentary organic matter accumulation and degradation controlled by productivity. Nature 364, 786–788.

Boussafir, M., Gelin, F., Lallier-Vergès, E., Derenne, S., Bertrand, P., Largeau, C., 1995. Electron microscopy and pyrolysis of kerogens from the Kimmeridge Clay Formation, UK: source organisms, preservation processes, and origin of microcycles. Geochimica et Cosmochimica Acta 59, 3731–3747.

Collister, J.W., Summons, R.E., Lichtfouse, E., Hayes, J.M., 1992. An isotopic biogeochemical study of the Green River oil shale. Organic Geochemistry 19, 265–276.

Cooper, B.S., Barnard, P.C., Telnaes, N., 1995. The Kimmeridge Clay Formation of the North Sea. In: Katz, B.J. (Ed.), Petroleum Source Rocks. Springer, Berlin, pp. 89–110.

Cox, B.M., Gallois, R.W., 1981. The stratigraphy of the Kimmeridge Clay of the Dorset type area and its correlation with some other Kimmeridge sequences. Reports of the Institute of Geological Science 80, 1–44.

Deines, P., 1980. The isotopic composition of reduced organic carbon. In: Fritz, P., Fontes, J.Ch. (Eds.), Handbook of Environmental Isotope Geochemistry. Elsevier, Amsterdam, pp. 329–406.

Doré, A.G., Vollset, J., Hamar, G.P., 1985. Correlation of the off shore sequences referred to the Kimmeridge Clay Formation: relevance to the Norwegian Sector. In: Thomas, B.M. (Ed.), Petroleum Geochemistry in Exploration on the Norwegian Shelf. Graham & Trotham, London, pp. 27–37.

de Leeuw, J.W., Largeau, C., 1993. A review of macromolecular organic compounds that comprise living organisms and their role in kerogen, coal and petroleum formation. Organic Geochemistry 21, 23–63.

Eglinton, T.I., Sinninghe Damsté, J.S., Kohnen, M.E.L., de Leeuw, J.W., 1990. Rapid estimation of the organic sulphur content of kerogens, coals and asphaltenes by pyrolysis-gas chromatography. Fuel 69, 1394–1404.

Hartgers, W.A., Sinninghe Damsté, J.S., de Leeuw, J.W., Ling, Y., Crelling, J.C., 1995. The influence of mineral matter on the separation of amorphous marine kerogens using density gradient centrifugation. Organic Geochemistry 23, 777–784.

Hartgers, W.A., Sinninghe Damsté, J.S., Requejo, A.G., Allan, J., Hayes, J.M., de Leeuw, J.W., 1994a. Evidence for only minor contributions from bacteria to sedimentary organic carbon. Nature 369, 224–227.

Hartgers, W.A., Sinninghe Damsté, J.S., Requejo, A.G., Allan, J., Hayes, J.M., Ling, Y., Xie, T.M., Primack, J., de Leeuw, J.W., 1994b. A molecular and carbon isotopic study towards the origin and diagenetic fate of diaromatic carotenoids. Organic Geochemistry 22, 703–725.

Hartnett, H.E., Keil, R.G., Hedges, J.I., Devol, A.H., 1998. Influence of oxygen exposure time on organic carbon preservation in continental margin sediments. Nature 391, 572–574.

Hedges, J.I., Sheng Hu, F., Devol, A.H., Hartnett, H.E., Tsamakis, E., Keil, R.G., 1999. Sedimentary organic matter preservation: a test for selective degradation under oxic conditions. American Journal of Science 299, 529–555.

Herbin, J.P., Müller, C., Geyssant, J.R., Mélières, F., Penn, I.E., The Yorkim Group, 1993. Variation of the distribution of organic matter within a transgressive system tract: Kimmeridge Clay (Jurassic), England. In: Katz, B.J., Pratt, L.M. (Eds.), Source Rocks in a Sequence Stratigraphic Framework, AAPG Studies in Geology #37. American Association of Petroleum Geologists, Tulsa, pp. 67–100.

Hernes, P.J., Hedges, J.I., Peterson, M.L., Wakeham, S.G., Lee, C., 1996. Neutral carbohydrate geochemistry of particulate material in the central equatorial Pacific. Deep-Sea Research, Part II 43, 1181–1204.

Hesselbo, S.P., Gröcke, D.R., Jenkyns, H.C., Bjerrum, C.J., Farrimond, P., Morgans Bell, H.S., Green, O.R., 2000. Massive dissociation of gas hydrate during a Jurassic oceanic anoxic event. Nature 406, 392–395.

Hesselbo, S.P., Robinson, S.A., Surlyk, F., Piasecki, S., 2002. Terrestrial and marine extinction at the Triassic–Jurassic boundary synchronized with major carbon-cycle perturbation: a link to initiation of massive volcanism. Geology 30, 251–254.

Hollander, D.J., McKenzie, J.A., Hsu, K.J., Huc, A.Y., 1993. Application of an eutrophic lake model to the origin of ancient organic-carbon-rich sediments. Global Biochemical Cycles 7, 157–179.

Huc, A.Y., Lallier-Vergès, E., Bertrand, P., Carpentier, B., Hollander, D.J., 1992. Organic matter response to change of depositional environment in Kimmeridgian shales, Dorset, UK. In: Whelan, J.K., Farrington, J.W. (Eds.), Organic Matter: Productivity, Accumulation and Preservation in Recent and Ancient Sediments. Columbia University Press, New York, pp. 469–486.

Kenig, F., Hayes, J.M., Popp, B.N., Summons, R.E., 1994. Isotopic biogeochemistry of the Oxford Clay Formation (Jurassic), UK. Journal of the Geological Society London 151, 139–152.

Kenig, F., Hudson, J., Sinninghe Damsté, J.S., Popp, B.N., 2004. High-frequency intermittent anoxia: reuniting a black-shale (Lower Oxford Clay, Callovian, U.K.) and its biofacies. Geology 32, 421–424.

Kohnen, M.E.L., Sinninghe Damsté, J.S., Rijpstra, W.I.C., de Leeuw, J.W., 1990. Alkylthiophenes as sensitive indicators of palaeoenvironmental changes: a study of a Cretaceous oil shale from Jordan. In: Orr, W.L., White, C.M. (Eds.), Geochemistry of Sulfur in Fossil Fuels, ACS Symposium Series, 429. American Chemical Society, Washington, DC, pp. 444–485.

Kok, M.D., Rijpstra, W.I.C., Robertson, L., Volkman, J.K., Sinninghe Damsté, J.S., 2000a. Early steroid sulfurisation in surface sediments of a permanently stratified lake (Ace Lake, Antarctica). Geochimica et Cosmochimica Acta 64, 1425–1436.

Kok, M.D., Schouten, S., Sinninghe Damsté, J.S., 2000b. Formation of insoluble, nonhydrolyzable, sulfur-rich macromolecules via incorporation of inorganic sulfur species into algal carbohydrates. Geochimica et Cosmochimica Acta 64, 2689–2699.

Koopmans, M.P., Köster, J., van Kaam-Peters, H.M.E., Kenig, F., Schouten, S., Hartgers, W.A., de Leeuw, J.W., Sinninghe Damsté, J.S., 1996. Diagenetic and catagenetic products of isorenieratene: molecular indicators for photic zone anoxia. Geochimica et Cosmochimica Acta 60, 4467–4496.

Kuhnt, W., Herbin, J.P., Thurow, J.W., Wiedmann, J., 1990. Distribution of Cenomanian–Turonian organic facies in the western Mediterranean and along the adjacent Atlantic Margin. AAPG Studies in Geology 30, 133–160.

Lallier-Vergès, E., Hayes, J.M., Boussafir, M., Zaback, D.A., Tribovillard, N.P., Connan, J., Bertrand, P., 1997. Productivity-induced sulphur enrichment of hydrocarbon-rich sediments from the Kimmeridge Clay Formation. Chemical Geology 134, 277–288.

Laws, E.A., Popp, B.N., Bidigare, R.R., Kennicutt, M.C., Macko, S.A., 1995. Dependence of phytoplankton carbon isotopic composition on growth rate and (CO_2)aq: theoretical considerations and experimental results. Geochimica et Cosmochimica Acta 59, 1131–1138.

Miller, R.G., 1989. A palaeoceanographic approach to the Kimmeridge Clay Formation. In: Huc, A.Y. (Ed.), Deposition of Organic facies, AAPG Studies in Geology #30. American Association of Petroleum Geologists, Tulsa, pp. 13–26.

Mongenot, T., Derenne, S., Largeau, C., Tribovillard, N.-P., Lallier-Vergès, E., Dessort, D., Connan, J., 1999. Spectroscopic, kinetic and pyrolytic studies of kerogen from the dark parallel laminae facies of the sulphur-rich Orbagnoux deposit (Upper Kimmeridgian, Jura). Organic Geochemistry 30, 39–56.

Moodley, L., Middelburg, J.J., Herman, P.M.J., Soetaert, K., de Lange, G.J., 2005. Oxygenation and organic-matter preservation in marine sediments: direct experimental evidence from ancient organic carbon-rich deposits. Geology 33, 889–892.

Morgans-Bell, H.S., Coe, A.L., Hesselbo, S.P., Jenkyns, H.C., Weedon, G.P., Marshall, J.E.A., Tyson, R.V., Williams, C.J., 2001. Integrated stratigraphy of the Kimmeridge Clay Formation (Upper Jurassic) based on exposures and boreholes in south Dorset, UK. Geological Magazine 138, 511–539.

Nijenhuis, I.A., Bosch, H.-J., Sinninghe Damsté, J.S., Brumsack, H.-J., de Lange, G.J., 1999. Organic matter and trace element-rich sapropels and black shales: a geochemical comparison. Earth and Planetary Science Letters 169, 277–290.

Oschmann, W., 1988. Kimmeridge clay sedimentation – a new cyclic model. Palaeogeography, Palaeoclimatology, Palaeoecology 65, 217–251.

Oschmann, W., 1991. Distribution, dynamics and palaeoecology of Kimmeridgian (Upper Jurassic) shelf anoxia in western Europe. In: Tyson, R.V., Pearson, T.H. (Eds.), Modern and Ancient Continental Shelf Anoxia, Geological Society Special Publication No. 58. Geological Society, London, pp. 381–395.

Pakulski, J.D., Benner, R., 1992. An improved method for the hydrolysis and MBTH analysis of dissolved and particulate carbohydrates in seawater. Marine Chemistry 40, 143–160.

Pancost, R.D., van Dongen, B.E., Esser, A., Morgans-Bell, H., Jenkyns, H.C., Sinninghe Damsté, J.S., 2005. Variation in organic-matter composition and its impact on organic-carbon preservation in the Kimmeridge Clay Formation (Upper Jurassic, Dorset, southern England). In: Harris, N.B. (Ed.), The Deposition of Organic-Carbon-Rich Sediments: Models, Mechanisms, and Consequences, SEPM Special Publication 82, pp. 261–278.

Popp, B.N., Laws, E.A., Bridigare, R.R., Dore, J.E., Hanson, K.L., Wakeham, S.G., 1998. Effect of phytoplankton cell geometry on carbon isotopic fractionation. Geochimica et Cosmochimica Acta 62, 69–77.

Ramanampisoa, L., Disnar, J.R., 1994. Primary control of palaeoproduction on organic matter preservation and accumulation in the Kimmeridge rocks of Yorkshire (UK). Organic Geochemistry 21, 1153–1167.

Riboulleau, A., Baudin, F., Deconinck, J.F., Derenne, S., Largeau, C., Tribovillard, N., 2003. Depositional conditions and organic matter preservation pathways in an epicontinental environment: the Upper Jurassic Kashpir Oil Shales (Volga Basin, Russia). Palaeogeography, Palaeoclimatology, Palaeoecology 197, 171–197.

Riboulleau, A., Derenne, S., Sarret, G., Largeau, C., Baudin, F., Connan, J., 2000. Pyrolytic and spectroscopic study of a sulphur-rich kerogen from the "Kashpir oil shales" (Upper Jurassic, Russian platform). Organic Geochemistry 31, 1641–1661.

Riboulleau, A., Mongenot, T., Baudin, F., Derenne, S., Largeau, C., 2002. Factors controlling the survival of proteinaceous material in Late Tithonian kerogens (Kashpir Oil Shales, Russia). Organic Geochemistry 33, 1127–1130.

Romankevich, E.A., 1978. Geochemistry of Organic Matter in the Ocean. Springer, Berlin.

Sælen, G., Tyson, R.V., Telnæs, N., Talbot, M.R., 2000. Contrasting watermass conditions during deposition of the Whitby Mudstone (Lower Jurassic) and Kimmeridge Clay (Upper Jurassic) formations, UK. Palaeogeography, Palaeoclimatology, Palaeoecology 163, 163–196.

Schouten, S., Baas, M., van Kaam-Peters, H.M.E., Sinninghe Damsté, J.S., 1998a. Long-chain 3-isopropyl alkanes: a new class of sedimentary acyclic hydrocarbons. Geochimica et Cosmochimica Acta 62, 961–964.

Schouten, S., Klein Breteler, W.C.M., Blokker, P., Schogt, N., Rijpstra, W.I.C., Grice, K., Baas, M., Sinninghe Damsté, J.S., 1998b. Biosynthetic effects on the stable carbon isotopic composition of algal lipids: implications for deciphering the carbon isotopic biomarker record. Geochimica et Cosmochimica Acta 62, 1397–1406.

Sinninghe Damsté, J.S., 1997. C_{27}–C_{30} neohop-13(18)-enes and their aromatic derivatives in sediments: indicators for water column stratification? Abstract. 18th International Meeting on Organic Geochemistry Maastricht, The Netherlands, pp. A659–A660.

Sinninghe Damsté, J.S., de Leeuw, J.W., 1992. Organically bound sulphur in coal: a molecular approach. Fuel Processing Technology 30, 109–178.

Sinninghe Damsté, J.S., de Las Heras, F.X.C., de Leeuw, J.W., 1992. Molecular analysis of sulphur-rich brown coals by flash pyrolysis-gas chromatography–mass spectrometry. The Type III-S kerogen. Journal of Chromatography 607, 361–376.

Sinninghe Damsté, J.S., de Las Heras, F.X.C., van Bergen, P.F., de Leeuw, J.W., 1993a. Characterization of Tertiary Catalan lacustrine oil shales: discovery of extremely organic sulphur-rich Type I kerogens. Geochimica et Cosmochimica Acta 57, 389–415.

Sinninghe Damsté, J.S., Kok, M.D., Köster, J., Schouten, S., 1998. Sulfurized carbohydrates and important sedimentary sink for organic carbon? Earth and Planetary Science Letters 164, 7–13.

Sinninghe Damsté, J.S., White, C.M., Green, J.B., de Leeuw, J.W., 1999. Organosulfur compounds in sulfur-rich Rasa coal. Energy and Fuels 13, 728–738.

Sinninghe Damsté, J.S., Schouten, S., van Duin, A.C.T., 2001a. Isorenieratene derivatives in sediments: possible controls on their distribution. Geochimica et Cosmochimica Acta 65, 1557–1571.

Sinninghe Damsté, J.S., van Dongen, B.E., Rijpstra, W.I.C., Schouten, S., Volkman, J.K., Geenevasen, J.A.J., 2001b. Novel intact glycolipids in sediments from an Antarctic lake (Ace Lake). Organic Geochemistry 32, 321–332.

Sinninghe Damsté, J.S., Wakeham, S.G., Kohnen, M.E.L., Hayes, J.M., de Leeuw, J.W., 1993b. A 6000-year sedimentary molecular record of chemocline excursions in the Black Sea. Nature 362, 827–829.

Sinninghe Damsté, J.S., Rijpstra, W.I.C., Coolen, M.J.L., Schouten, S., Volkman, J.K., 2006. Timing of the early sulfurization of highly branched isoprenoid (HBI) alkenes in sulfidic Holocene sediments from Ellis Fjord, Antarctica. Organic Geochemistry, submitted.

Sirevåg, R., Ormerod, J.G., 1970. Carbon dioxide fixation in green sulphur bacteria. Journal of Biochemistry 120, 399–408.

Skoog, A., Benner, R., 1997. Aldoses in various size fractions of marine organic matter: implications for carbon cycling. Limnology and Oceanography 42, 1803–1813.

Summons, R.E., Powell, T.G., 1986. Chlorobiaceae in Palaeozoic seas revealed by biological markers, isotopes and geology. Nature 319, 763–765.

Tribovillard, N., Bialkowski, A., Tyson, R.V., Lallier-Verges, E., Deconick, J.F., 2001. Organic facies variation in the late Kimmeridgian of the Boulonnais area (northernmost France). Marine Petroleum Geology 18, 371–389.

Tyson, R.V., 1989. Late Jurassic palynofacies trends, Piper and Kimmeridge Clay Formations, UK onshore and northern North Sea. In: Batter, D.J., Keen, H.C. (Eds.), Northwest European Micropalaeontology and Palynology. Ellis Horwood, Chichester, pp. 135–172.

Tyson, R.V., 1995. Sedimentary Organic Matter. Chapman & Hall, London.

Tyson, R.V., 1996. Sequence-stratigraphical interpretation of organic facies variations in marine siliciclastic systems: general principles and application to the onshore Kimmeridge Clay Formation, UK. In: Hesselbo, S.P., Parkinson, D.N. (Eds.), Sequence Stratigraphy in British Geology Geological Society Special Publications. Geological Society, London, pp. 75–96.

Tyson, R.V., 2004. Variation in marine total organic carbon through the type Kimmeridge Clay Formation (Late Jurassic), Dorset, UK. Journal of the Geological Society 161, 667–673.

Tyson, R.V., Wilson, R.C.L., Downie, C., 1979. A stratified water column environmental model for the type Kimmeridge Clay. Nature 277, 377–380.

van Breugel, Y., Schouten, S., Paetzel, M., Ossebaar, J., Sinninghe Damsté, J.S., 2005. Reconstruction of $\delta^{13}C$ of chemocline CO_2 (aq) in past oceans and lakes using the $\delta^{13}C$ of fossilized isorenieratene. Earth and Planetary Science Letters 235, 421–434.

van der Meer, M.T.J., Schouten, S., Sinninghe Damsté, J.S., 1998. The effect of the reversed tricarboxylic acid cycle on the ^{13}C contents of bacterial lipids. Organic Geochemistry 28, 527–533.

van Dongen, B.E., Schouten, S., Sinninghe Damsté, J.S., 2002. Carbon isotope variability in monosaccharides and lipids of aquatic and terrestrial plants. Marine Ecology Progress Series 232, 83–92.

van Dongen, B.E., Schouten, S., Baas, M., Geenevasen, J.A.J., Sinninghe Damsté, J.S., 2003a. An experimental study on the low temperature sulfurization of carbohydrates. Organic Geochemistry 34, 1129–1144.

van Dongen, B.E., Schouten, S., Sinninghe Damsté, J.S., 2003b. Sulfurization of carbohydrates results in a S-rich, unresolved complex mixture in kerogen pyrolysates. Energy and Fuels 17, 1109–1118.

van Kaam-Peters, H.M.E., Sinninghe Damsté, J.S., 1997. Characterisation of an extremely organic sulphur-rich, 150 Ma old carbonaceous rock: palaeoenvironmental implications. Organic Geochemistry 27, 371–397.

van Kaam-Peters, H.M.E., Schouten, S., Köster, J., Sinninghe Damsté, J.S., 1998. Controls on the molecular and carbon isotopic composition of organic matter deposited in a Kimmeridgian euxinic shelf sea: evidence for preservation of carbohydrates through sulfurisation. Geochimica et Cosmochimica Acta 62, 3259–3283.

van Kaam-Peters, H.M.E., Schouten, S., Sinninghe Damsté, J.S., 1997. A molecular and carbon isotope biogeochemical study of biomarkers and kerogen pyrolysates of the Kimmeridge Clay facies: palaeoenvironmental implications. Organic Geochemistry 27, 399–422.

Volkman, J.K., Maxwell, J.R., 1986. Acyclic isoprenoids as biological markers. In: Johns, R.B. (Ed.), Biological Markers in the Sedimentary Record. Elsevier, New York, pp. 1–42.

Weedon, G.P., Coe, A.L., Gallois, R.W., 2004. Cyclostratigraphy, orbital tuning and inferred productivity for the type Kimmeridge Clay (Late Jurassic), Southern England. Journal of the Geological Society 161, 655–666.

Wehausen, R., Brumsack, H.-J., 2000. Chemical cycles in Pliocene sapropel-bearing and sapropel-barren eastern Mediterranean sediments. Palaeogeography, Palaeoclimatology, Palaeoecology 158, 325–352.

Werne, J.P., Hollander, D.J., Behrens, A., Schaeffer, P., Albrecht, P., Sinninghe Damsté, J.S., 2000. Timing of early diagenetic sulfurization of organic matter: a precursor–product relationship in Holocene sediments of the anoxic Cariaco Basin, Venezuela. Geochimica et Cosmochimica Acta 64, 1741–1751.

Wignall, P.B., 1994a. Black Shales. Clarendon Press, Oxford.

Wignall, P.B., 1994b. Mudstone lithofacies in the Kimmeridge Clay Formation, Wessex Basin, Southern England: implications for the origin and controls of the distribution of mudstone – discussion. Journal of Sedimentary Research A64, 927–929.

Williams, P.F.V., Douglas, A.G., 1980. A preliminary organic geochemical investigations of the Kimmeridge oil shales. In: Douglas, A.G., Maxwell, J.R. (Eds.), Advances in Organic Geochemistry 1979. Pergamon, Oxford, pp. 531–545.

Williams, P.F.V., Douglas, R.G., 1983. The effects of lithologic variation on organic geochemistry in the Kimmeridge Clay of Britain. In: Bjorøy, M. et al. (Eds.), Advances in Organic Geochemistry 1981. Wiley, Chichester, pp. 568–575.